AD-A253 417

US Army Corps
of Engineers

COMPUTER-AIDED STRUCTURAL
ENGINEERING (CASE) PROJECT

TECHNICAL REPORT ITL-92-4

# INTRODUCTION TO THE COMPUTATION OF RESPONSE SPECTRUM FOR EARTHQUAKE LOADING

by

Robert M. Ebeling

Information Technology Laboratory

DEPARTMENT OF THE ARMY
Waterways Experiment Station, Corps of Engineers
3909 Halls Ferry Road, Vicksburg, Mississippi   39180-6199
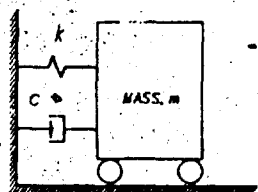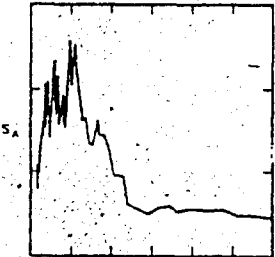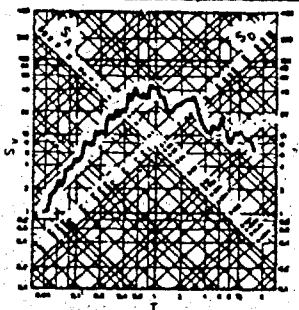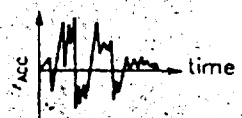
DTIC
ELECTE
JUL 1 6 1992
S C D

92-18846

June 1992
Final Report

Approved For Public Release; Distribution Is Unlimited

Prepared for DEPARTMENT OF THE ARMY
US Army Corps of Engineers
Washington, DC   20314-1000

REPORT DOCUMENTATION PAGE

Form Approved
OMB No. 0704-0188

1. AGENCY USE ONLY (Leave blank)	2. REPORT DATE June 1992	3. REPORT TYPE AND DATES COVERED Final report

4. TITLE AND SUBTITLE

Introduction to the Computation of Response Spectrum
for Earthquake Loading

5. FUNDING NUMBERS

6. AUTHOR(S)

Robert M. Ebeling

7. PERFORMING ORGANIZATION NAME(S) AND ADDRESS(ES)

USAE Waterways Experiment Station, Information
Technology Laboratory, 3909 Halls Ferry Road, Vicksburg,
MS 39180-6199

8. PERFORMING ORGANIZATION REPORT NUMBER

Technical Report
ITL-92-4

9. SPONSORING/MONITORING AGENCY NAME(S) AND ADDRESS(ES)

DEPARTMENT OF THE ARMY
US Army Corps of Engineers
Washington, DC 20314-1000

10. SPONSORING/MONITORING AGENCY REPORT NUMBER

11. SUPPLEMENTARY NOTES

Available from National Technical Information Service, 5285 Port Royal Road,
Springfield, VA 22161

12a. DISTRIBUTION/AVAILABILITY STATEMENT

Approved for public release; distribution is unlimited

12b. DISTRIBUTION CODE

13. ABSTRACT (Maximum 200 words)

This technical report presents an introduction to the computation of a
linear response spectrum for earthquake loading and defines the terms associated
with response spectra. A response spectrum is a graphical relationship of
maximum values of acceleration, velocity, and/or displacement response of an
infinite series of elastic single degree of freedom (SDOF) systems subjected to
time dependent dynamic excitation.

This report reviews the formulation and solution of the equation of motion
for a damped linear SDOF system subjected to time dependent dynamic excitation.
Due to the irregular nature of the acceleration time histories that have been
recorded during earthquakes, numerical methods are used to compute the response
of SDOF systems during the course of developing response spectra. The
fundamentals of the solution of the equation of motion for SDOF systems are also
described.

14. SUBJECT TERMS Dynamics Earthquake engineering Response spectra			15. NUMBER OF PAGES 61
			16. PRICE CODE

17. SECURITY CLASSIFICATION OF REPORT	18. SECURITY CLASSIFICATION OF THIS PAGE	19. SECURITY CLASSIFICATION OF ABSTRACT	20. LIMITATION OF ABSTRACT
UNCLASSIFIED	UNCLASSIFIED	UNCLASSIFIED	

PREFACE

This report presents an introduction to the computation of response spectrum for earthquake loading. This study is part of the work entitled "Design Response Spectra For Structures" sponsored by the Civil Works Guidance Update Program, Headquarters, US Army Corps of Engineers (HQUSACE). Funds for publication of the report were provided from those available for the Computer-Aided Structural Engineering Program managed by the Information Technology Laboratory (ITL). Technical Monitor for the project is Mr. Lucian Guthrie, HQUSACE.

The work was performed at the US Army Engineer Waterways Experiment Station (WES) by Dr. Robert M. Ebeling, Interdisciplinary Research Group, Computer-Aided Engineering Division (CAED), ITL. This report was prepared by Dr. Ebeling with review commentary provided by Professor William P. Dawkins of Oklahoma State University, Mr. Barry Fehl, CAED, ITL, Mr. Maurice Power of Geomatrix Consultants and Dr. Yusof Ghanaat of QUEST Structures. This study is part of a general investigation on design response spectra for hydraulic structures under the direction of Dr. Ebeling. All work was accomplished under the general supervision of Dr. N. Radhakrishnan, Director, ITL.

At the time of publication of this report, Director of WES was Dr. Robert W. Whalin. Commander and Deputy Director was COL Leonard G. Hassell, EN.

1

CONTENTS

LIST OF TABLES

LIST OF FIGURES

4

CONVERSION FACTORS, NON-SI TO SI (METRIC)
UNITS OF MEASUREMENT

Non-SI units of measurement used in this report can be converted to SI (metric) units as follows:

Multiply	By	To Obtain
degrees (angle)	0.01745329	radians
cycles per second	1.0	hertz
cycles per second	6.28318531	radians per second
feet	0.3048	meters
inches	2.54	centimeters
acceleration of gravity (standard)	980.665	centimeters/second/second
	32.174	feet/second/second
	386.086	inches/second/second
gal	1.0	centimeters/second/second
feet/second/second	30.4838	centimeters/second/second
pounds	4.4822	newtons
tons	8.896	kilonewtons

INTRODUCTION TO THE COMPUTATION OF RESPONSE SPECTRUM
FOR EARTHQUAKE LOADING

PART I: INTRODUCTION

1. This paper presents an introduction to the computation of a response spectrum for earthquake loading. A response spectrum is a graphical relationship of maximum values of acceleration, velocity, and/or displacement response of an infinite series of elastic single degree of freedom (SDOF) systems subjected to a time dependent excitation. To accomplish this task, the formulation and solution of the equation of motion for a damped SDOF system subjected to dynamic excitation is reviewed prior to discussion of the response spectrum.

2. Examples of idealized SDOF systems are shown in Figure 1. The dynamic excitation may be due to the forcing function P(t) (Figure 1c) acting on the mass or to ground shaking, typically expressed in terms of a ground acceleration time history, as shown in Figure 2. The dynamic response of damped SDOF systems is described by the variations of displacement, velocity, and acceleration of the mass with time. A plot of the maximum values of acceleration, velocity, and/or displacement of an infinite series of SDOF systems versus undamped natural period is called a response spectrum.

3. The response spectrum is the cornerstone of modern earthquake engineering and structural dynamics. It is used to calculate the dynamic response of multi-degree of freedom (MDOF) semidiscrete structural models of buildings and hydraulic structures (i.e. dams, locks, and intake towers) as well as for the evaluation of frequency content of recorded accelerograms. The frequency content of accelerograms is of importance for selecting the ground motion(s) to be used as the forcing functions in the dynamic analysis.

4. The damped SDOF system and the dynamic equilibrium equation for the system are introduced in Part II. The derivation of the equation of motion for a damped SDOF system subjected to a time dependent force history is described in Part III. Part IV derives the equation of motion for the case of a damped SDOF system subjected to earthquake shaking. This part also describes how the earthquake shaking problem may be reformulated as an equivalent force history problem.

6
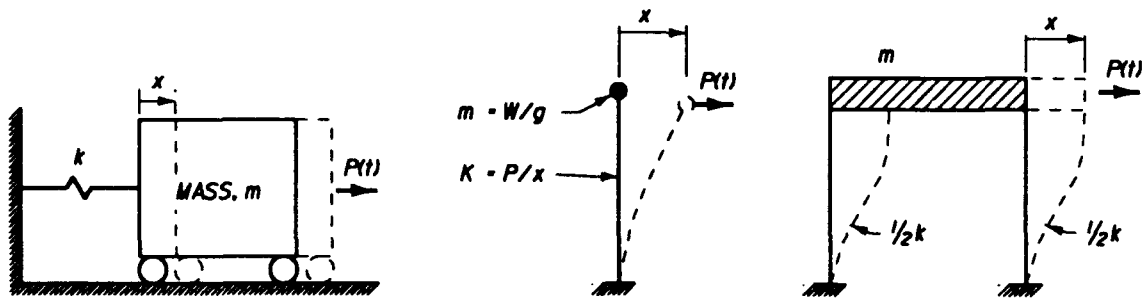
(a) Idealized rigid mass SDOF systems
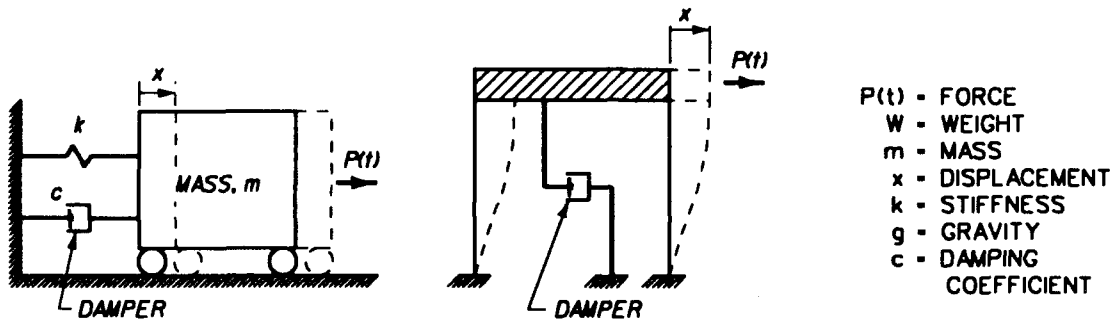
P(t) - FORCE
W - WEIGHT
m - MASS
x - DISPLACEMENT
k - STIFFNESS
g - GRAVITY
c - DAMPING
COEFFICIENT

(b) Idealized damped SDOF systems
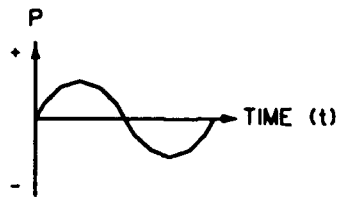
(c) Variation in force with time

Figure 1. Idealized single degree of freedom (SDOF) systems

7
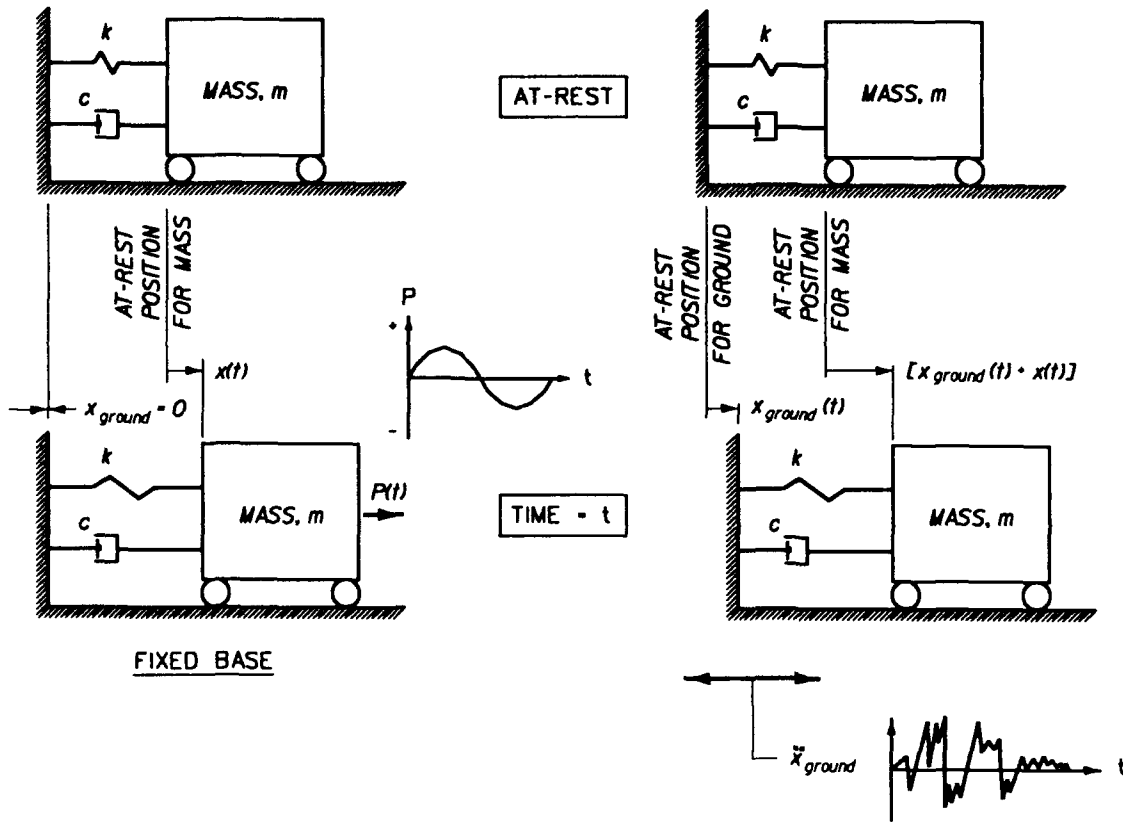
(a) Damped SDOF response to external force P(t)

(b) Damped SDOF response to ground acceleration $\ddot{x}_{ground}(t)$

Figure 2. Dynamic response of two damped SDOF systems

5.   The fundamentals of the solution of the equation of motion using numerical procedures are introduced in Part V.   Because of the irregular nature of the acceleration time histories that have been recorded during earthquakes, numerical methods are used to compute the response of SDOF systems for developing response spectra.

6.   Part VI describes the construction of response spectra using the accelerations, velocities, and displacements obtained from the numerical integration of the equations of motion for an infinite series of SDOF systems subjected to earthquake shaking.   The terms associated with response spectra are also defined in Part VI.

PART II: THE DYNAMIC EQUILIBRIUM EQUATION FOR A DAMPED SDOF SYSTEM

7. A damped SDOF system consists of a rigid mass m, a linear spring of stiffness k, and a viscous damper with damping coefficient c, as shown in Figure 2. The viscous damper represents the energy absorbing component of the system. Each rigid mass is constrained to move in the horizontal x direction. The SDOF system in Figure 2a is subjected to a time dependent horizontal force history P(t), while the SDOF system in Figure 2b is shaken by a time dependent horizontal ground acceleration, $\ddot{x}_{ground}(t)$. The double overdot represents the second derivative of displacement x with respect to time. The dynamic response of either system at any time t is governed by the relationship

$$\Sigma\, F(t) = m\, \ddot{x}_{total}(t) \tag{1}$$

where

$\ddot{x}_{total}(t)$ — the acceleration of the mass m.

8. In earthquake engineering problems, the displacements, velocities and accelerations of the rigid mass differ from those of the ground (Figure 2b). It is convenient to describe the motion of the rigid mass in terms of the relative displacement of the mass with respect to the ground as

$$x(t) = x_{total}(t) - x_{ground}(t) \tag{2}$$

where

$x(t)$ — the relative displacement

$x_{total}(t)$ — the displacement of the mass from its at-rest position

$x_{ground}(t)$ — the displacement of the ground

The relative velocity and relative acceleration of the mass m at time t are obtained by differentiation of Equation 2

$$\dot{x}(t) = \dot{x}_{total}(t) - \dot{x}_{ground}(t) \tag{3}$$

and

$$\ddot{x}(t) = \ddot{x}_{total}(t) - \ddot{x}_{ground}(t) \tag{4}$$

The solutions to the two dynamic problems shown in Figure 2 are described in Part III for an applied dynamic force and in part IV for an earthquake excitation.

10

PART III: ORDINARY DIFFERENTIAL EQUATION FOR A DAMPED SDOF SYSTEM - FORCED VIBRATIONS

9. This part describes the derivation of the ordinary differential equation of second order that governs the dynamic response of the damped SDOF system shown in Figure 3 to a time dependent external force P(t). This simple mechanical system serves as an introduction to the fundamentals of the dynamics of a SDOF system and as background information for the dynamic problem involving a SDOF system undergoing a time dependent ground acceleration as described in Part IV.

10. Assume that at time t, P(t) acts in the positive x direction (to the right) and that the acceleration, velocity, and displacement of the mass are positive. For this problem, the ground is at-rest (i.e. $x_{ground} = 0$), therefore $x_{total}(t)$ is equal to x(t). The movement of the mass from its at-rest position to the right stretches the spring, resulting in a restoring force $f_k(t)$. For a linear spring

$$f_k(t) = k \, x(t) \tag{5}$$

where

       k = the spring stiffness

       x(t) = the displacement of the mass at time t

Similarly, the restoring force $f_c(t)$ contributed by the viscous damper at time t is given by

$$f_c(t) = c \, \dot{x}(t) \tag{6}$$

where

       c = the damping coefficient

       $\dot{x}(t)$ = the velocity of the mass at time t

Both $f_k(t)$ and $f_c(t)$ act in the negative x direction (to the left) at time t, tending to restore the mass to its at-rest position (refer to Figure 3). The sum of forces acting on the mass, the left-hand-side of Equation 1, is

$$\Sigma \, F(t) = P(t) - f_k(t) - f_c(t) \tag{7}$$

Substituting Equations 5, 6, and 7 into Equation 1 with $\ddot{x}(t) = \ddot{x}_{total}(t)$ and rearranging results in
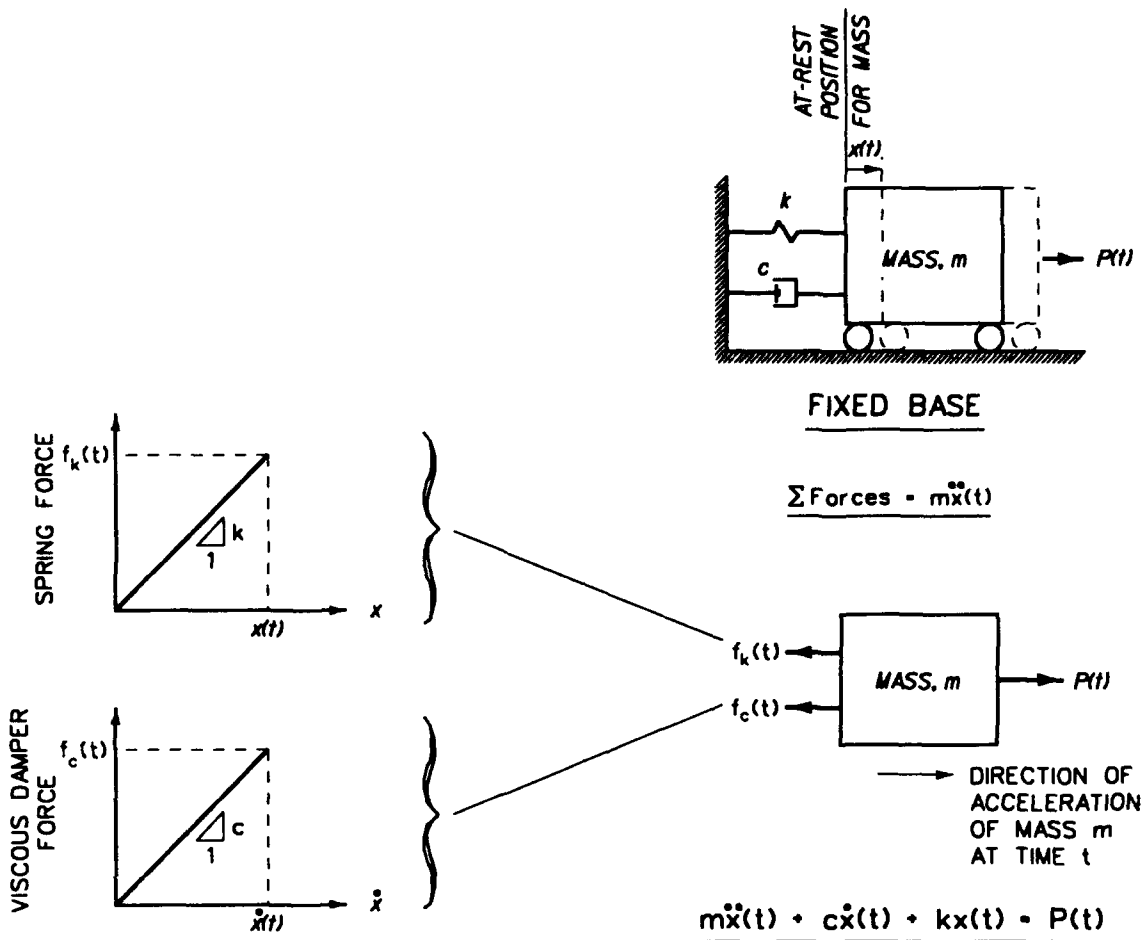
Figure 3. Forces acting on a linear SDOF system at time t, external force P(t) applied

$$m\,\ddot{x}(t) + c\,\dot{x}(t) + k\,x(t) = P(t) \qquad (8)$$

The first term in Equation 8 represents the inertial force $f_i(t)$, associated with the mass m undergoing an acceleration $\ddot{x}(t)$, which acts opposite to the direction of the acceleration of the mass m (refer to Figure 4).

Free Vibration

11. Free vibration results from the application of an initial displacement and/or velocity with no external forcing function acting on the system $(P(t) = 0)$.
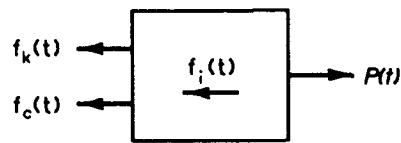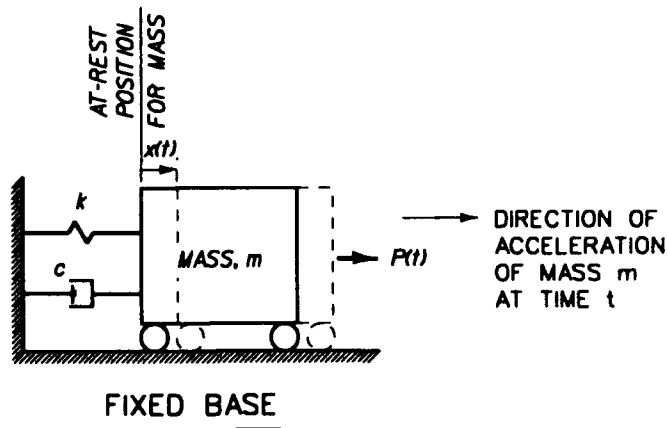
$$f_i(t) + f_c(t) + f_k(t) = P(t)$$

where the inertial force f_i is given by:

$$f_i(t) = m\ddot{x}(t)$$

Figure 4. Inertial force acting opposite to the acceleration of mass m at time t, external force P(t) applied

Undamped Free Vibration

12. The equation of motion (Equation 8) for an undamped system (c = 0) in free vibration is

$$m\ddot{x}(t) + k\,x(t) = 0 \tag{9}$$

and its solution is

$$x(t) = x_o \cos \omega t + \frac{\dot{x}_o}{\omega} \sin \omega t \tag{10}$$

where

x_o = the initial displacement

$\dot{x}_o$ = the initial velocity

13

and

$$\omega = \sqrt{\frac{k}{m}}$$
(11)

where

ω — constant circular frequency (rad/sec).

Equation 10 is obtained using standard solution procedures for linear differential equations, such as the method of undetermined coefficients (Section 2.12 in Kreyszig 1972). The motion described by Equation 10 and shown in Figure 5a is cyclic with a constant maximum amplitude

$$|x(t)|_{max} = \sqrt{x_o^2 + \left[\frac{\dot{x}_o}{\omega}\right]^2}$$
(12)

and constant circular frequency ω. The cyclic nature of vibration may also be expressed in terms of the natural period of vibration , T (sec), of the undamped SDOF system as

$$T = \frac{2\pi}{\omega}$$
(13)

or the natural cyclic frequency of vibration f (cycles/sec or Hz) where

$$f = \frac{1}{T} = \frac{\omega}{2\pi}$$
(14)

13. Figure 6 shows the computed response of a SDOF system with k = 1 N/m and mass m = 1 kg, subjected to an initial displacement x_o = 1 cm ($\dot{x}_o$ = 0).* The circular frequency is equal to 1 radian/sec (by equation 11) and the undamped natural period of vibration is equal to 2π seconds. Plots of the displacement, velocity and acceleration of the mass for the first cycle of harmonic response are shown in Figure 6, as well as the variation with time of the spring force and inertial force acting on the rigid mass. Note that the inertial force acts opposite to the direction of the acceleration vector for the rigid mass.

---

* One newton, N, is the force which gives an acceleration of 1 m/sec^2 to a mass of 1 kg.

14

$$\ddot{x} + \omega^2 x = 0$$

PERIOD OF VIBRATION: $T = 2\pi \sqrt{m/K}$

{ INITIAL DISPLACEMENT x_o AT $t=0$
{ INITIAL VELOCITY $\dot{x}_o$ AT $t=0$

$$x = x_o \cos \omega t + \frac{\dot{x}_o}{\omega} \sin \omega t \qquad \text{where: } \omega = \sqrt{\frac{k}{m}}$$

(a) Undamped free vibration

$$\ddot{x} + 2\beta\omega \dot{x} + \omega^2 x = 0$$

PERIOD OF VIBRATION: $T_D = T / \sqrt{1-\beta^2}$

{ INITIAL DISPLACEMENT x_o AT $t=0$
{ INITIAL VELOCITY $\dot{x}_o$ AT $t=0$

EXPONENTIAL DECAY OF MAX. AMPLITUDE

$$x = e^{-\beta\omega t}\left\{ x_o \cos\omega_D t + \left[\frac{\dot{x}_o + \beta\omega x_o}{\omega_D}\right] \sin \omega_D t \right\}$$

$$\text{where: } \omega_D = \omega\sqrt{1-\beta^2}$$
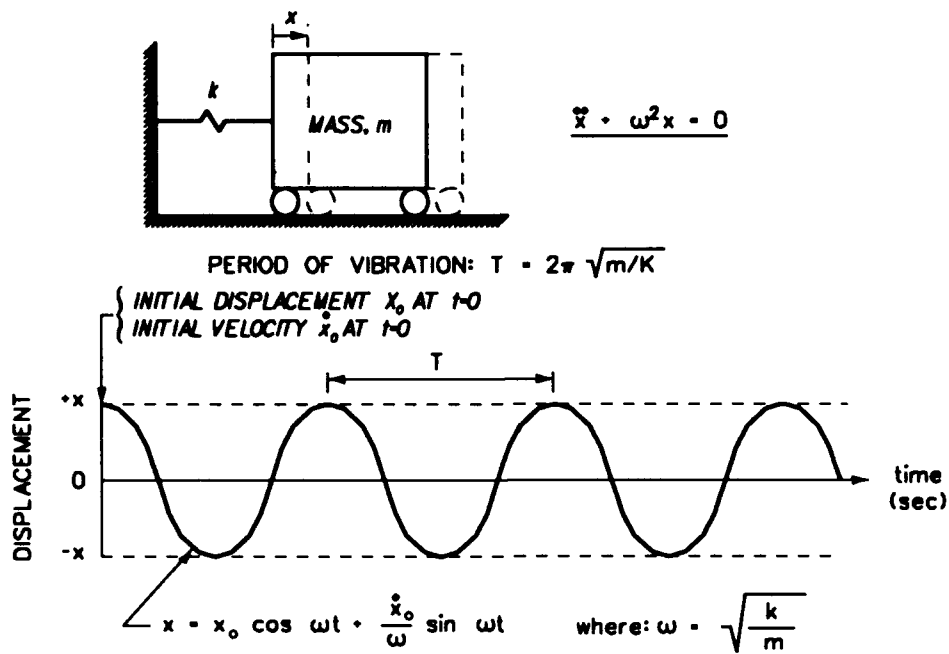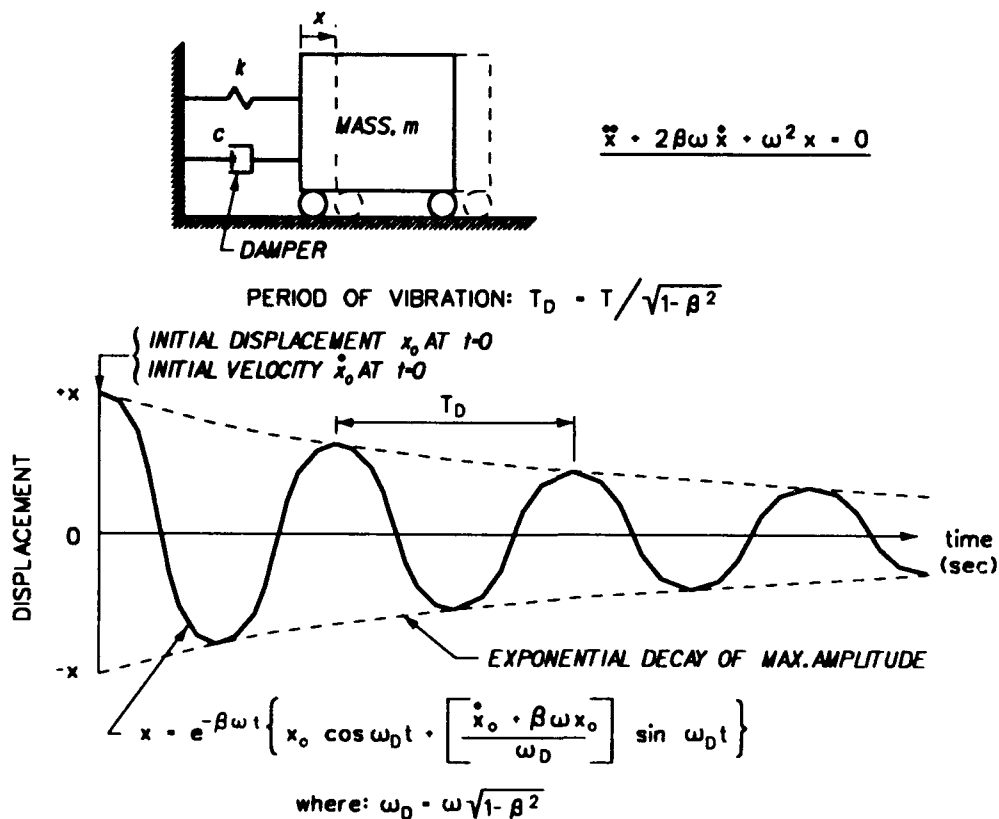
(b) Damped free vibration (damped at a ratio to critical damping equal to β)

Figure 5. Free vibration response of damped and undamped SDOF systems

15
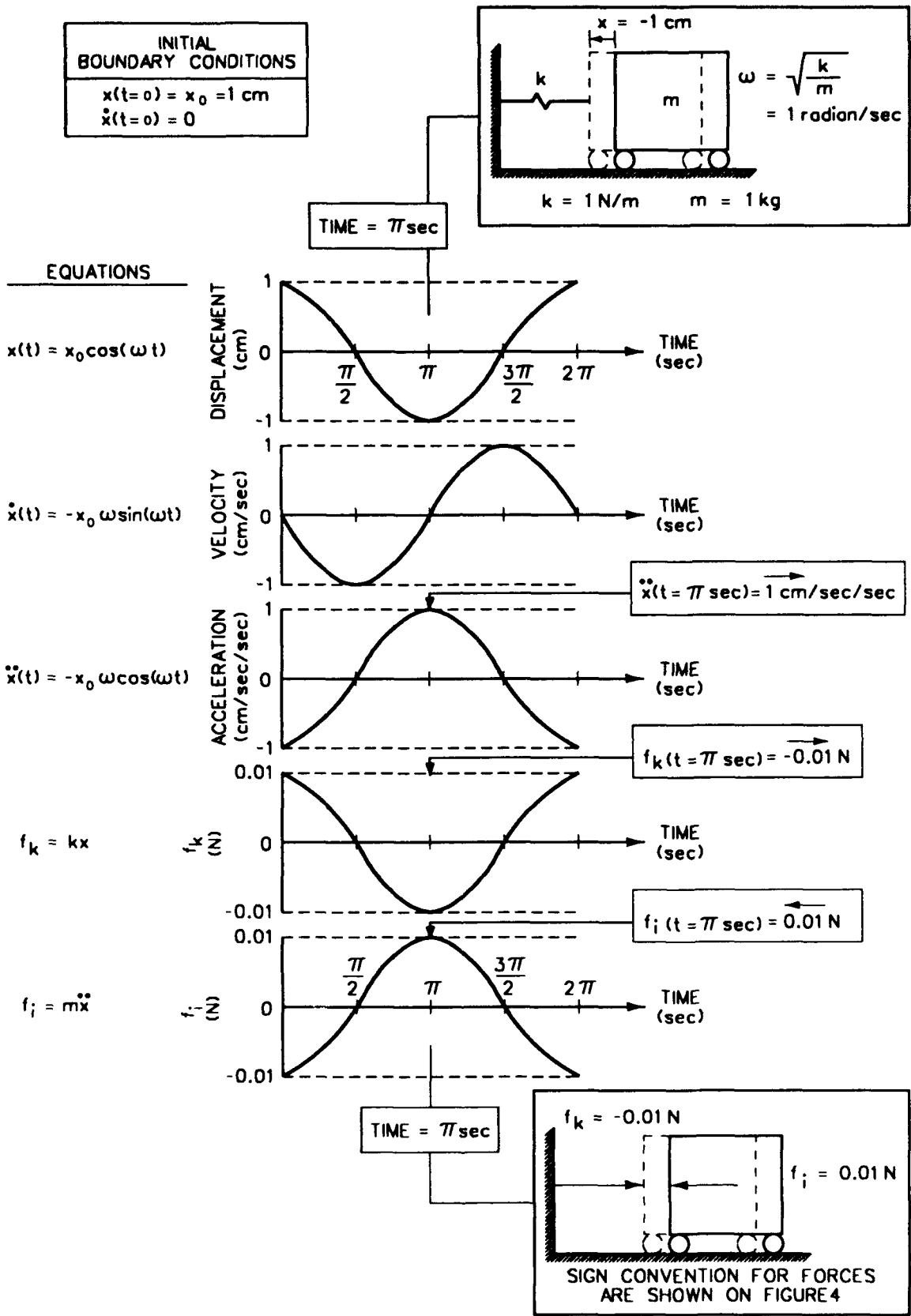
Figure 6. Undamped free vibration responses of a SDOF system given an initial displacement of 1 cm

16

Damped Free Vibration

14. The equation of motion for damped free vibration may be written as

$$\ddot{x}(t) + 2\beta\omega\dot{x}(t) + \omega^2 x(t) = 0 \tag{15}$$

where

$$\beta = \frac{c}{2\,m\,\omega} \tag{16}$$

Equation 15 was derived from Equation 8 by (1) dividing each term by the mass m, (2) introducing the constant β for the damping force term, and (3) $P(t)$ set equal to zero. The solution of Equation 15 is, for $\beta < 1$,

$$x(t) = e^{-\beta\omega t}\left\{ x_o \cos\omega_D t + \left[\frac{\dot{x}_o + \beta\omega x_o}{\omega_D}\right]\sin\omega_D t \right\} \tag{17}$$

The motion described by Equation 17 for $\beta < 1$, shown in Figure 5b, is periodic with an exponentially decaying amplitude and damped circular frequency

$$\omega_D = \omega\sqrt{1 - \beta^2} \tag{18}$$

or period

$$T_D = \frac{T}{\sqrt{1 - \beta^2}} \tag{19}$$

where ω and T are the circular frequency and period of the undamped system, respectively.

15. When $\beta = 1$ the period of the damped system becomes infinite indicating that the motion is no longer cyclic but after an initial maximum displacement, decays exponentially without subsequent reversal of direction. A system with $\beta = 1$ or with damping

$$c = c_{critical} = 2\,m\,\omega \tag{20}$$

is said to be "critically" damped. Hence

17

$$\beta = \frac{c}{c_{critical}} = \frac{c}{2\,m\,\omega} \qquad (21)$$

is called the "damping ratio" or the "fraction of critical damping."
Typically for structures β is less than 0.1 and for material damping in soils
is less than 0.25. β may also be expressed as percentage. For typical struc-
tural systems the periods (or frequency) of the damped and undamped systems
are approximately equal, i.e.

$$T \approx T_D \qquad (22)$$

Forced Vibration with Dynamic Force Applied to Mass

16. The equation of motion (Equation 8) for the SDOF system (Figure 3)
may be written as

$$\ddot{x}(t) + 2\,\beta\,\omega\,\dot{x}(t) + \omega^2\,x(t) = \frac{P(t)}{m} \qquad (23)$$

In general there are three approaches to the solution of Equation 23: closed
form solutions, Duhamel's Integral, and numerical methods.

Closed Form Solutions

17. For a simple harmonic force history, such as $P(t)$ — Constant·sin
$[\omega_{drive}\cdot t]$ in Equations 8 and 23, closed form solutions are available in numer-
ous textbooks on both mechanical vibrations and structural dynamics. This
procedure is not practical for earthquake engineering problems involving
irregular force time histories.

Duhamel's Integral

18. A second procedure used to solve for the dynamic response of a SDOF
system involves the representation of the load time history $P(t)$ as a series

of impulse loadings P(τ) that are applied to the SDOF system for infinitesimal time intervals dτ, as shown in Figure 7.

dT - TIME INTERVAL
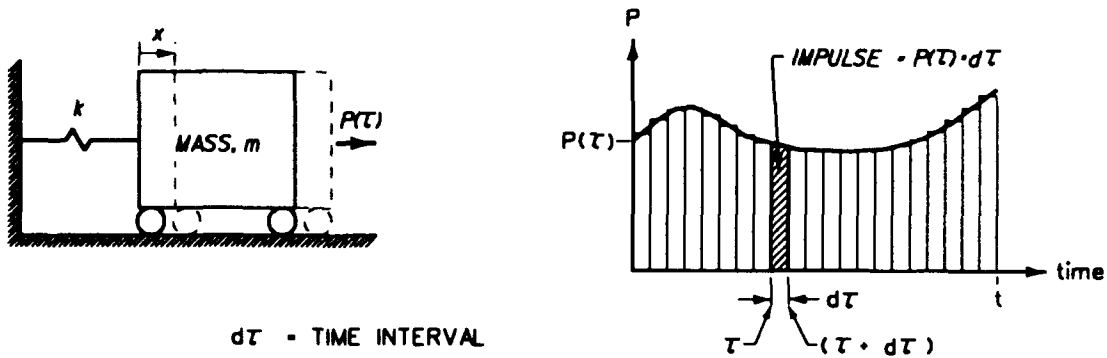
Figure 7. Load time history P(τ) as impulse loading to undamped SDOF
system

19.   Figures 8a through 8c outline the derivation of the incremental displacement dx of an undamped SDOF system at time t to a single force pulse P(τ)·dτ. Figure 8d gives the resulting integral solution, known as the Duhamel's integral, for the displacement of the undamped SDOF system at time t to the succession of force pulses applied between time - 0 and time - t.

20.   Duhamel's integral for a damped SDOF system is

$$x(t) = \frac{1}{m \omega_D} \int_0^t P(\tau) \, e^{-\beta\omega(t-\tau)} \sin [\omega_D(t - \tau)] \, d\tau \qquad (24)$$

where

ω_D - the damped circular frequency of vibration (Equation 18),

ω - the undamped circular frequency of vibration (Equation 11)

β - the fraction of critical damping (Equation 21).

21.   For a select few load time histories P(t), the integral may be evaluated directly. Irregular force time histories require numerical solutions to be used to evaluate Duhamel's integral. These procedures are described in numerous textbooks on structural dynamics.

Numerical Methods

22.   For most earthquake engineering problems, numerical methods are used to solve a form of Equation 8 or Equation 23 due to the irregular form of force time histories. Numerical methods will be discussed in Part V.

$P(T)dT = m(d\dot{x})$ or $d\dot{x} = \dfrac{1}{m}P(T)dT$
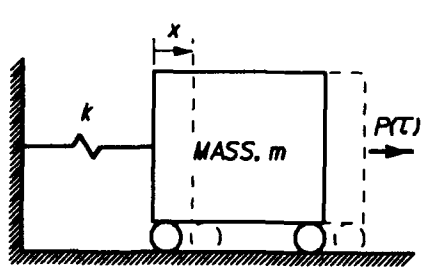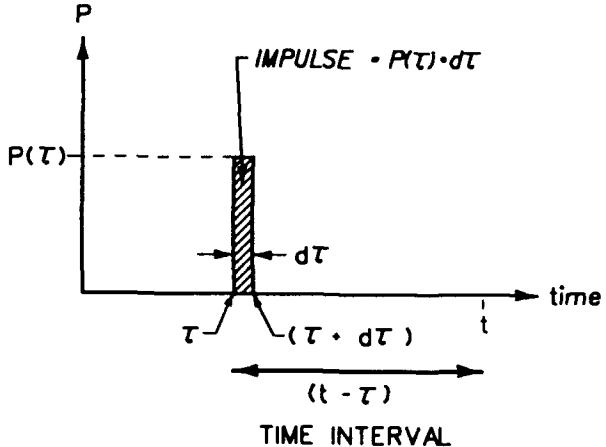
$d\dot{x} = $ INCREMENTAL VELOCITY $= \dot{x}_0(T)$

(a) Incremental velocity d$\dot{x}$ at time τ

$m\ddot{x} + kx = 0$

INITIAL CONDITIONS: $x(t=0) = 0$
$\dot{x}(t=0) = \dot{x}_0$

EXACT SOLUTION: $x = \dfrac{\dot{x}_0}{\omega}\sin \omega t$

where: $\omega = \sqrt{\dfrac{k}{m}}$
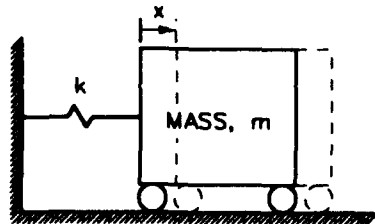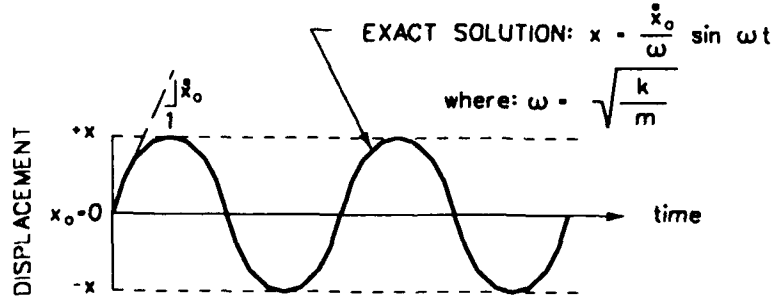
(b) Exact solution for free vibration response
(undamped)

Figure 8.   Duhamel's integral for an undamped SDOF
system

20

Introducing $d\dot{x}$ from (o) into $\dot{x}_0$ of (b), the incremental displacement is given by

$$dx(t) = \frac{1}{\omega}\left[\frac{1}{m}P(\tau)d\tau\right]\sin\left[\omega(t-\tau)\right]$$

(c) Incremental displacement at time t due to a single pulse at time τ

$$x(t) = \int_0^t dx(t)\,d\tau$$

$$x(t) = \frac{1}{m\omega}\int_0^t P(\tau)\sin\left[\omega(t-\tau)\right]d\tau$$

(d) Duhamel's integral

Figure 8. (Continued).

PART IV: ORDINARY DIFFERENTIAL EQUATION FOR A DAMPED SDOF SYSTEM - GROUND ACCELERATION

23. This part describes the derivation of the ordinary differential equation of second order that governs the dynamic response of the damped SDOF system shown in Figure 2b shaken by a horizontal ground acceleration $\ddot{x}_{ground}(t)$. $\ddot{x}_{ground}$ varies in both magnitude and direction with time. Assume that at time t, $\ddot{x}_{ground}(t)$ is positive (to the right) and the acceleration, velocity, and displacement of the mass are positive. The restoring forces of the spring and dashpot shown in Figure 9 are given by Equations 5 and 6, respectively. Combination of Equation 1

$$\sum F(t) = m\ddot{x}_{total}(t) \tag{1}$$

Equation 5

$$f_k(t) = k\, x\,(t) \tag{5}$$

and Equation 6

$$f_c(t) = c\, \dot{x}(t) \tag{6}$$

result in

$$m\, \ddot{x}_{total}(t) + c\, \dot{x}(t) + k\, x(t) = 0 \tag{25}$$

where $\dot{x}$ and x are relative velocity and displacement of the mass (Equations 2 and 3) valid at any time t. The first term in Equation 19 represents the inertial force f_i, associated with the mass m undergoing a total acceleration $\ddot{x}_{total}(t)$. This force vector acts opposite to the direction of the total acceleration vector of the mass m, as shown in Figure 9. Substituting Equation 4 into Equation 25 for $\ddot{x}_{total}$ results in the expression

$$m\, \ddot{x}(t) + c\, \dot{x}(t) + k\, x = -\, m\, \ddot{x}_{ground}(t) \tag{26}$$

or

$$\ddot{x}(t) + 2\, \beta\, \omega\, \dot{x}(t) + \omega^2\, x(t) = -\, \ddot{x}_{ground}(t) \tag{27}$$

22

AT-REST

TIME - t

$[x_{total}(t) = x_{ground}(t) + x(t)]$

$x_{ground}(t)$

DIRECTION OF
ACCELERATION
OF MASS m
AT TIME t

$\ddot{x}_{ground}$ time

$f_k(t)$

$f_c(t)$

$f_i(t)$
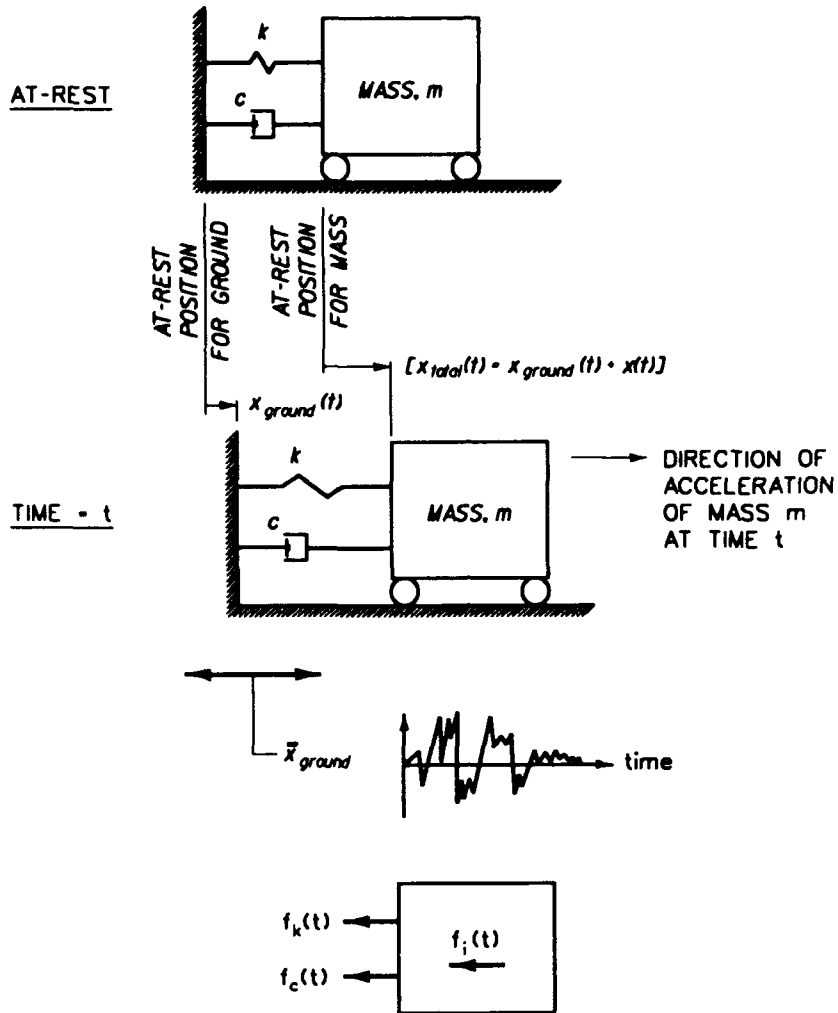
$$f_i(t) + f_c(t) + f_k(t) = 0$$

WHERE:

$$f_i(t) = m\ddot{x}_{total}(t)$$

$$= m[\ddot{x}_{ground}(t) + \ddot{x}(t)]$$

Figure 9. Forces acting on an SDOF system at time t,
ground acceleration $\ddot{x}_{ground}$

where

ω = the undamped circular frequency (Equation 11)

β = the damping ratio (Equation 21)

The terms associated with the relative movement of the mass are collected on
the left-hand-side of the equal sign. Either differential equation

23

(Equation 25 or 26) describes the dynamic response of a damped SDOF system shaken by a horizontal ground acceleration $\ddot{x}_{ground}$.

Equivalent SDOF Problems

24.   Comparison of Equation 26 with Equation 8 shows that the relationships for the two SDOF systems shown in Figure 2 differ by the term on the right-hand-side of the equal sign (the force history). Thus, the problem of a damped SDOF system shaken by a time varying ground acceleration is equivalent to the problem of a damped SDOF system resting on a fixed base and subjected to a time dependent force P(t) of magnitude - m·$\ddot{x}_{ground}$, as shown in Figure 10.

GROUND ACCELERATION

FIXED BASE
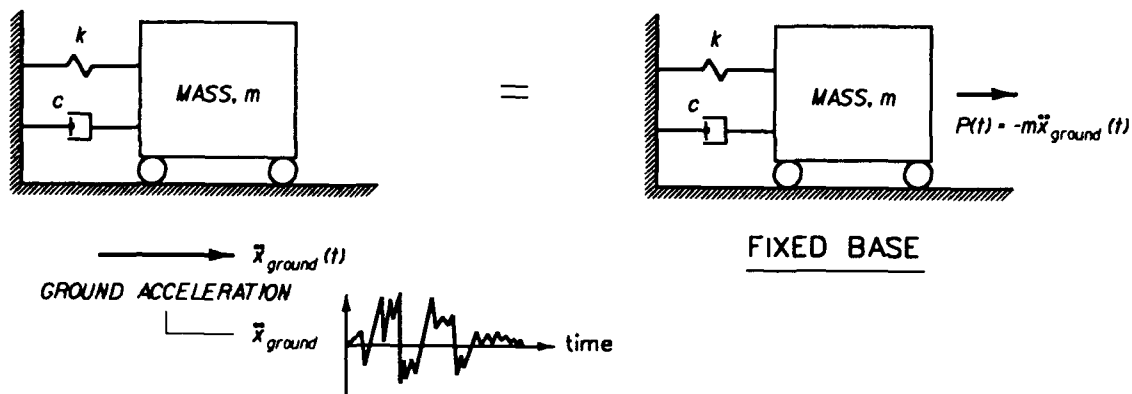
STEP 1, SOLVE

$$m\ddot{x}(t) + c\dot{x}(t) + kx(t) = -m\ddot{x}_{ground}(t)$$

STEP 2, SOLVE

$$\ddot{x}_{total}(t) = \ddot{x}(t) + \ddot{x}_{ground}(t)$$

Figure 10. Equivalent dynamic SDOF system problems

Solution of the Equation of Motion

25.   The total dynamic response of the SDOF system problem is computed in two steps. Step 1 solves for the relative response of the damped SDOF system as governed by the ordinary differential Equation 27, and in Step 2, the total response is equal to the sum of the relative response (from step 1) plus the motion of the ground.

Closed Form Solutions

26. For simple harmonic ground accelerations (e.g. $\ddot{x}_{ground}$ = Constant·sin [ω_{drive}· t]) closed form solutions to Equation 27 are available in numerous textbooks on both mechanical vibrations and structural dynamics. This procedure is impractical for earthquake engineering problems due to the irregular nature of ground acceleration time histories.

Duhamel's Integral

27. A second procedure used to solve for the relative displacement of the SDOF system involves the representation of the load time history P(t) = -m$\ddot{x}_{ground}$(t) as a series of impulse loadings P(τ) applied to the SDOF system for infinitesimal time intervals dτ (Figure 7). By introducing P(t) = -m$\ddot{x}_{ground}$(t) into Equation 24, Duhamel's integral for a damped SDOF system is

$$x(t) = - \frac{1}{\omega_D} \int_0^t \ddot{x}_{ground}(\tau) \; e^{-\beta\omega(t-\tau)} \; \sin \; [\omega_D(t - \tau)] \; d\tau \qquad (28)$$

where

ω_D = the damped angular frequency of vibration (Equation 18)

ω = the undamped angular frequency of vibration (Equation 11)

β = the fraction of critical damping (Equation 16)

The irregular forms of acceleration time histories require numerical solutions to be used to evaluate Duhamel's integral.

Numerical Methods

28. In usual applications to earthquake engineering problems, numerical methods are used to solve Equation 27 or Equation 28 for the relative displacement of the SDOF mass because of the irregular nature of ground acceleration time histories (discussed in Part V).

PART V: SOLUTION OF DYNAMIC EQUILIBRIUM EQUATIONS FOR A DAMPED SDOF SYSTEM USING NUMERICAL METHODS

29. This part introduces the fundamentals of numerical methods used to solve for the accelerations, velocities, and displacements of a damped SDOF system due to a time dependent loading. In general, there are two categories of numerical methods used for solving the dynamic equilibrium equation: direct integration methods and frequency-domain methods. This part discusses direct integration methods only. The reader is referred to books on structural dynamics for a description of frequency-domain methods.

Direct Integration Methods

30. Direct integration methods are used to solve for the response of the SDOF (and MDOF semidiscrete structural models) by direct integration of the dynamic equilibrium equations at closely spaced, discrete time intervals throughout the time of shaking using a numerical step-by-step procedure of analysis. The term "direct" means that prior to numerical integration, there is no transformation of the equations into a different form, as is done in a frequency-domain analysis. Table 1 lists some of the step-by-step algorithms used in structural dynamics for both SDOF systems and MDOF semidiscrete structural models and in the characterization of ground motions for earthquake engineering problems.

31. Direct integration methods are based on two concepts. First, the equation of motion (Equation 27) is satisfied at discrete points in time (i.e. t, $t + \Delta t$, ...) during earthquake shaking, and second, the forms of the variation in displacements, velocities, and accelerations within each time interval, Δt, are assumed. Direct integration time methods are classified as either explicit integration methods or implicit integration methods. The explicit integration method solves for the unknown values of $x_{t + \Delta t}$, $\dot{x}_{t + \Delta t}$, and $\ddot{x}_{t + \Delta t}$ at each new time $(t + \Delta t)$ using the equation of motion at time t, with the known values for x_t, $\dot{x}_t$, and $\ddot{x}_t$ at time t as the initial conditions. The implicit integration method solves for the unknown values of $x_{t + \Delta t}$, $\dot{x}_{t + \Delta t}$ and $\ddot{x}_{t + \Delta t}$ at each new time $(t + \Delta t)$ using the equation of motion at time $(t + \Delta t)$. For MDOF systems implicit schemes require the solution of a set of simultaneous linear equations, whereas explicit schemes involve the solution

Table 1

Step-by-Step Algorithms Used in Structural Dynamics

Family of Structural Dynamics Algorithms	Example of Algorithm	Type	Stability Condition	Order of Accuracy
collocation methods	Wilson-θ	Implicit	unconditional for $\theta > 1.366$	$O(\Delta t)^2$
Newmark-β methods	Average acceleration (trapezoidal rule)	Implicit	unconditional*	$O(\Delta t)^2$
	Linear acceleration	Implicit	conditional	$O(\Delta t)^2$
	Fox-Goodwin formula	Implicit	conditional	$O(\Delta t)^2$
	Central difference	Explicit	conditional	$O(\Delta t)^2$*
Houbolt's method		Implicit	unconditional	$O(\Delta t)^2$
α-method	Hilber-Hughes-Taylor	Implicit	unconditional*	$O(\Delta t)^2$
	Wood-Bossak-Zienkiewicz	Implicit	unconditional*	$O(\Delta t)^2$
θ_1-method	Hoff-Pahl	Implicit	unconditional*	$O(\Delta t)^2$
beta-m method	Katona-Zienkiewicz	Implicit	unconditional*	$O(\Delta t)^2$

* For select values of constants used in algorithm.

of a set of linear equations, each of which involves a single unknown. Both implicit and explicit step-by-step algorithms are listed in Table 1. Implicit algorithms are the more popular of the two types of numerical methods in earthquake engineering problems because of the larger size time step that may be used in the analysis. However, implicit methods involve considerable computational effort at each time step compared to explicit methods since the coefficient matrices for MDOF systems must be formulated, stored, and manipulated using matrix solution procedures.

27

Linear Acceleration Method

32. The principles common to all step-by-step time integration solutions of the equations of motions are illustrated for the Figure 10 SDOF system by applying the linear acceleration algorithm to this problem for a single time interval Δt. The dynamic response of the mass to an earthquake time history at each time step is expressed in terms of the values for the displacement, the velocity, and the acceleration of the mass.

33. The linear acceleration algorithm, one of the simpler forms of the Newmark-β family of implicit algorithms, assumes a linear variation in acceleration of the mass from time t to time (t + Δt) as shown in Figure 11. The values for the three variables are known at time t, and the values are unknown at time (t + Δt).

34. The assumed linear variation in acceleration provides one of the four equations used in the linear acceleration algorithm. The slope is expressed in terms of the values of acceleration at time t and time (t + Δt), as listed in Figure 11. Two additional equations are provided by twice integrating the linear acceleration relationship from time t to time (t + Δt). This results in a quadratic variation in velocity of the mass over time step Δt and a cubic variation in displacements of the mass over time Δt (Figure 11). The fourth equation is given by the equation of motion at time (t + Δt).

35. Figure 12 summarizes the three steps when solving for the dynamic response of the mass at each new time (t + Δt). The three relationships shown in this figure were obtained by rearranging the four relationships listed in Figure 10. The first stage of the analysis involves the application of the step-by-step procedure of analysis during the time of earthquake shaking, computing the time histories of response for the mass. Due to the nature of the formulation, the computed acceleration time history is the relative acceleration of the mass. The total acceleration of mass is equal to the sum of the relative acceleration values computed at each time step, and the corresponding ground acceleration values (step 2 in Figure 10).

Time Step

36. The selection of the size of the time step Δt to be used in the step-by-step calculation of the dynamic response of the SDOF (and of MDOF

Acceleration, $\dfrac{d^2x}{dt^2}$

LINEAR

$\ddot{x}_t$ $\ddot{x}_{t+\Delta t}$

assumed slope of

$$\left(\frac{\Delta\ddot{x}}{\Delta t}\right) = \frac{\ddot{x}_{t+\Delta t} - \ddot{x}_t}{\Delta t}$$

Velocity, $\dfrac{dx}{dt}$

QUADRATIC

$\dot{x}_t$ $\dot{x}_{t+\Delta t}$

Displacement, x

CUBIC

x_t $x_{t+\Delta t}$

t   TIME   t+Δt

Equation of motion

$$\Sigma F = m\ddot{x}$$
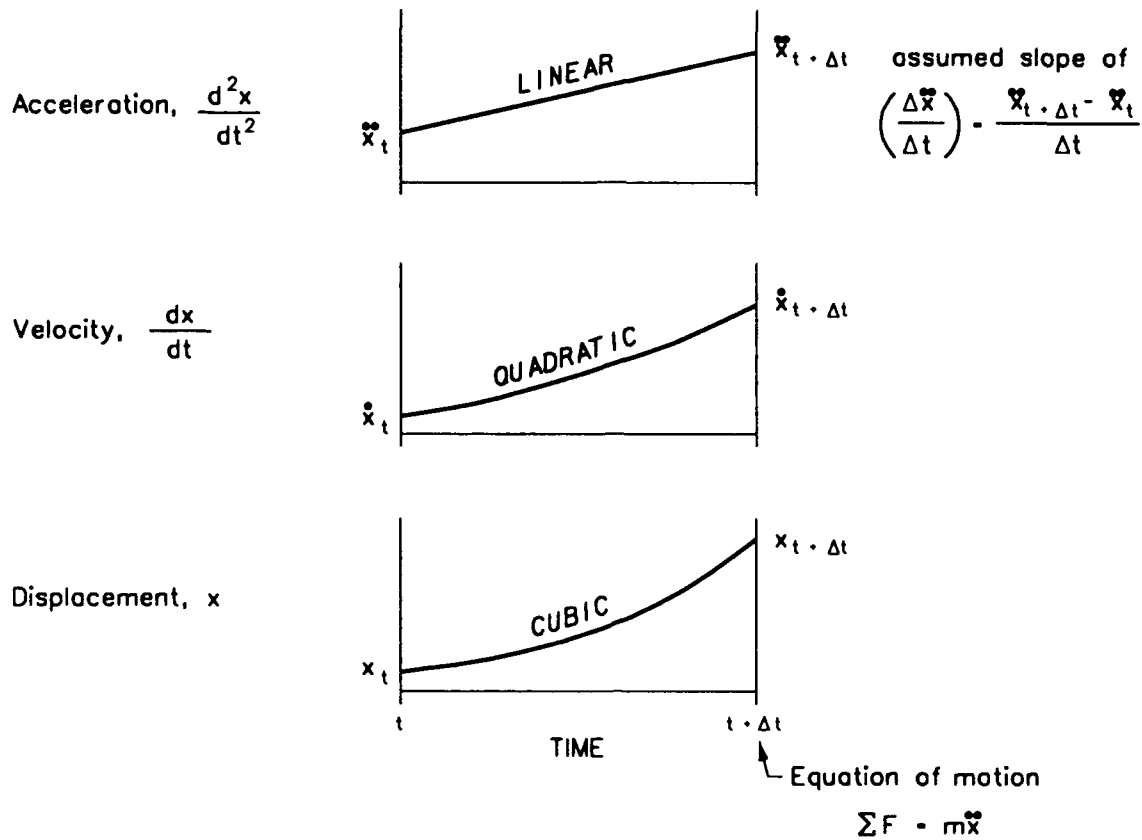
Variable	Known Value (time = t)	Unknown Value (time = t + Δt)
acceleration	$\ddot{x}_t$	$\ddot{x}_{t+\Delta t}$
velocity	$\dot{x}_t$	$\dot{x}_{t+\Delta t}$
displacement	x_t	$x_{t+\Delta t}$

Basic Equations:

$$m\ddot{x}_{t+\Delta t} + c\dot{x}_{t+\Delta t} + kx_{t+\Delta t} = P_{t+\Delta t}$$

linear accelerations,

$$\ddot{x}_{t+\Delta t} = \ddot{x}_t + \left(\frac{\Delta\ddot{x}}{\Delta t}\right)\Delta t$$

quadratic velocities,

$$\dot{x}_{t+\Delta t} = \dot{x}_t + \ddot{x}_t \Delta t + \frac{1}{2}\left(\frac{\Delta\ddot{x}}{\Delta t}\right)[\Delta t]^2$$

cubic displacements,

$$x_{t+\Delta t} = x_t + \dot{x}_t \Delta t + \frac{1}{2}\ddot{x}_t [\Delta t]^2 + \frac{1}{6}\left(\frac{\Delta\ddot{x}}{\Delta t}\right)[\Delta t]^3$$

Figure 11. Step-by-step time integration solution of the equation of motion using the linear acceleration method

29

$$\underline{LHS} \text{ (unknown)} \quad = \quad \underline{RHS} \text{ (known)}$$

step 1, solve $\quad constant_{LHS} \cdot x_{t+\Delta t} = constant_{RHS}$

step 2, solve for $\quad \dot{x}_{t+\Delta t} = \left[\dfrac{3}{\Delta t}\right] x_{t+\Delta t} - term_1$

step 3, solve for $\quad \ddot{x}_{t+\Delta t} = \left[\dfrac{6}{(\Delta t)^2}\right] x_{t+\Delta t} - term_2$

where the constants are given by

$$constant_{LHS} = k + \left[\dfrac{3}{\Delta t}\right] c + \left[\dfrac{6}{(\Delta t)^2}\right] m$$

$$constant_{RHS} = P_{t+\Delta t} + c \cdot term_1 + m \cdot term_2$$

and

$$P_{t+\Delta t} = - m \, \ddot{x}_{ground}(t + \Delta t)$$

$$term_1 = \left[\dfrac{3}{\Delta t}\right] x_t + 2 \, \dot{x}_t + \left[\dfrac{\Delta t}{2}\right] \ddot{x}_t$$

$$term_2 = \left[\dfrac{6}{(\Delta t)^2}\right] x_t + \left[\dfrac{6}{\Delta t}\right] \dot{x}_t + 2 \, \ddot{x}_t$$

Figure 12. Solution for the dynamic response of the mass at time
(t + Δt) using the linear acceleration algorithm

semidiscrete structural models) is restricted by stability and accuracy con-
siderations. The primary requirement of a numerical algorithm is that the
computed response converge to the exact response as $\Delta t \rightarrow 0$ (Hughes 1987). The
stability and accuracy criteria are expressed in terms of a maximum allowable
size for the time step, $\Delta t_{critical}$, which differs among the various numerical
algorithms.

Stability

37. The stability condition requirements for numerical algorithms are
categorized as either unconditional or conditional (Table 1). Bathe and
Wilson (1976), Bathe (1982), and Hughes (1987) describe an integration method
as unconditionally stable if the numerical solution for any initial value
problem (e.g. Figure 5a) does not grow without bound for any time step Δt,
especially if the time step is large. The method is conditionally stable if
the previous statement is true only for those cases in which Δt is less than
some critical time step $\Delta t_{critical}$. The stability criterion for a numerical
algorithm is established by the values assigned to the constants that are used
in the algorithm and the terms associated with the structural model (Hughes
and Belytshko 1983, Hughes 1987, and Dokainish and Subbaraj 1989). For
example, numerical stability considerations for the linear acceleration method
require that the time step Δt of a SDOF system be restricted to values given
by the relationship

$$\Delta t \leq \Delta t_{critical} \qquad (29)$$

where

$$\Delta t_{critical} = \frac{2\pi}{\omega} \frac{\sqrt{3}}{\pi} = \frac{1}{f} \frac{\sqrt{3}}{\pi} = T \frac{\sqrt{3}}{\pi} \qquad (30)$$

The values of $\Delta t_{critical}$ are summarized in Hughes and Belytshko (1983), Hughes
(1987), and Dokainish and Subbaraj (1989) for other algorithms.

38. The attributes of a stable numerical analysis are illustrated using
the free vibration problem of an undamped SDOF system shown in Figure 13,
given an initial displacement x_0 and an initial velocity $\dot{x}_0$. With no damping,
the exact solution for this initial value problem is a harmonic function that

31
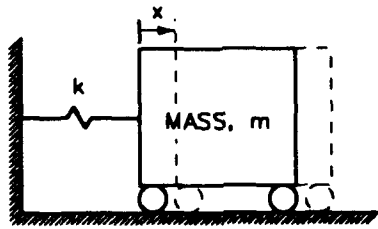
$$m\ddot{x} + kx = 0$$

INITIAL CONDITIONS: $x(t=0) = x_o$
$\dot{x}(t=0) = \dot{x}_o$

EXACT SOLUTION: $x = x_o \cos \omega t + \dfrac{\dot{x}_o}{\omega} \sin \omega t$

where: $\omega = \sqrt{\dfrac{k}{m}}$
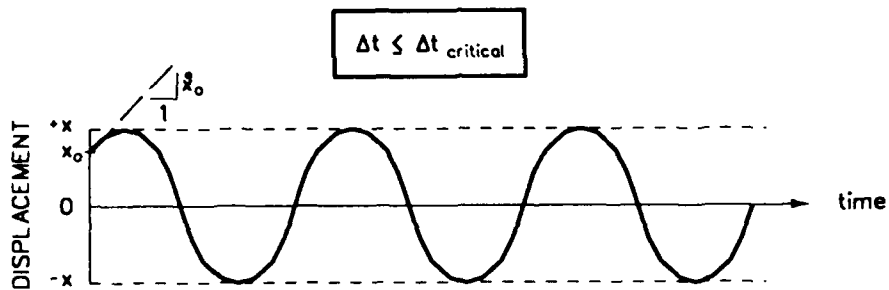
$\Delta t \leq \Delta t_{critical}$

(a) Stable free vibration response with a smaller time step than the critical time step
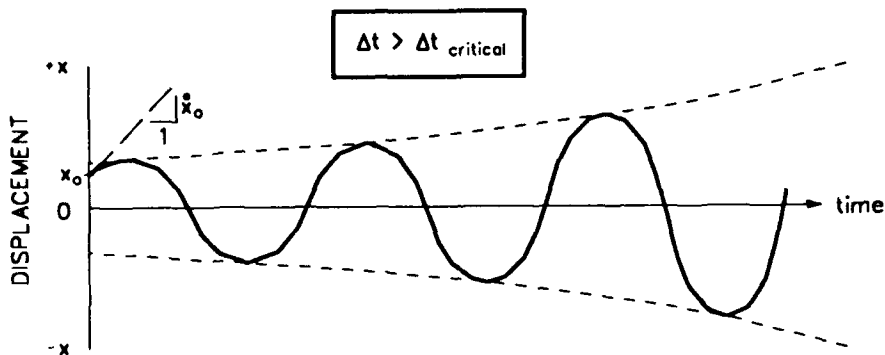
$\Delta t > \Delta t_{critical}$

(b) Unstable free vibration response due to a larger time step than the critical time step

Figure 13. Example of unstable response for an undamped SDOF system in free vibration

32

is continuous with time and equal to the sum of a sine wave plus a cosine wave of constant maximum amplitude. Figure 13a shows a conditionally stable numerical solution that corresponds to the exact solution. Figure 13a results contrast with Figure 13b results for the unstable free vibration response computed using $\Delta t > \Delta t_{critical}$, in which the maximum computed amplitude of the SDOF system increases with time.

39. The value of $\Delta t_{critical}$ for MDOF systems is governed by the smallest period or the largest frequency of the semidiscrete MDOF model. Violation of the stability criterion by an even single mode will destabilize the numerical solution of the dynamic problem. To avoid this restriction and increase the time step size, unconditionally stable integration methods are used.

Accuracy

40. The accuracy of a numerical algorithm is associated with the rate of convergence of the computed response to the exact response as $\Delta t \rightarrow 0$ (Hughes 1987). For the dynamic analysis of MDOF semidiscrete structural models using the finite element method, the accuracy of an algorithm is also concerned with the question of the computed response of spurious higher (frequency) modes of the semidiscrete model of the structural system. In general, accuracy considerations require a smaller time step for implicit algorithms, as compared to the stability requirements. For explicit methods, stability requirements usually dictate the maximum time step size.

41. Bathe and Wilson (1976) describe one approach used to assess the accuracy of numerical algorithm. Illustrated in Figure 14 is a free vibration problem of an undamped SDOF system subjected to an initial displacement x_0 and an initial velocity. x Figure 14a shows the exact solution to be harmonic with constant maximum amplitude. Figure 14b illustrates results for the free vibration response computed using a numerical algorithm. The errors in Figure 14b computed results take the form of amplitude decay with time and period elongation with time, as described in Figure 14c. The order of accuracy of numerical algorithms listed in Table 1 varies in proportion to the square of the time step used in the calculations.

42. One approach for selecting the value for the time step to be used in the calculations is to require a prescribed level of accuracy for the computed results. This decision process may be assisted by referring to charts developed for simplified SDOF system problems which define the magnitude of

EXACT SOLUTION: $x = x_0 \cos \omega t + \dfrac{\dot{x}_0}{\omega} \sin \omega t$

where: $\omega = \sqrt{\dfrac{k}{m}}$
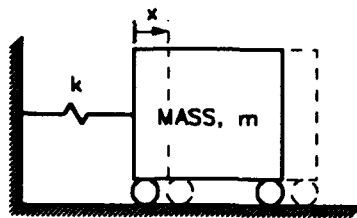
$m\ddot{x} + kx = 0$

INITIAL CONDITIONS: $x(t=0) = x_0$
$\dot{x}(t=0) = \dot{x}_0$
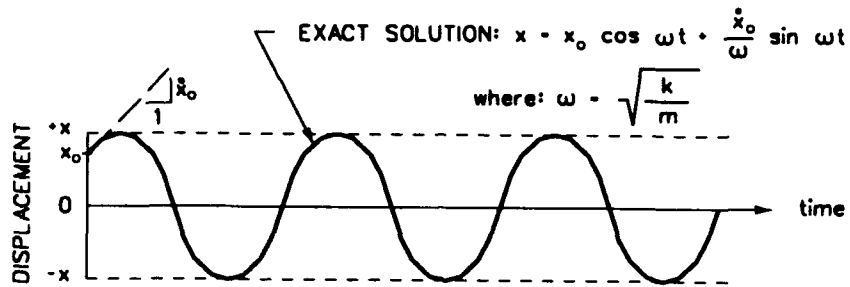
(a) Exact solution for free vibration response
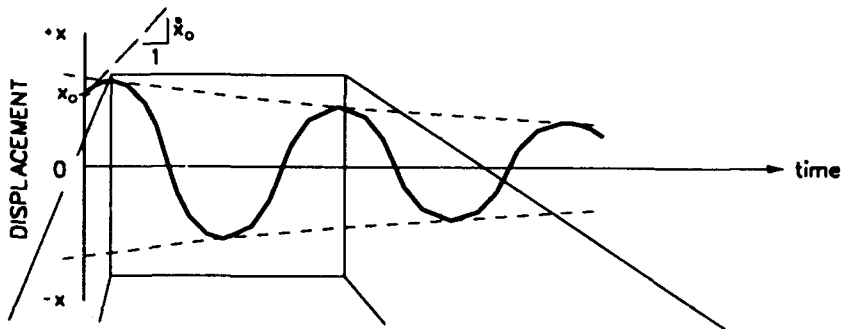
(b) Inaccurate free vibration response due to a
large time step
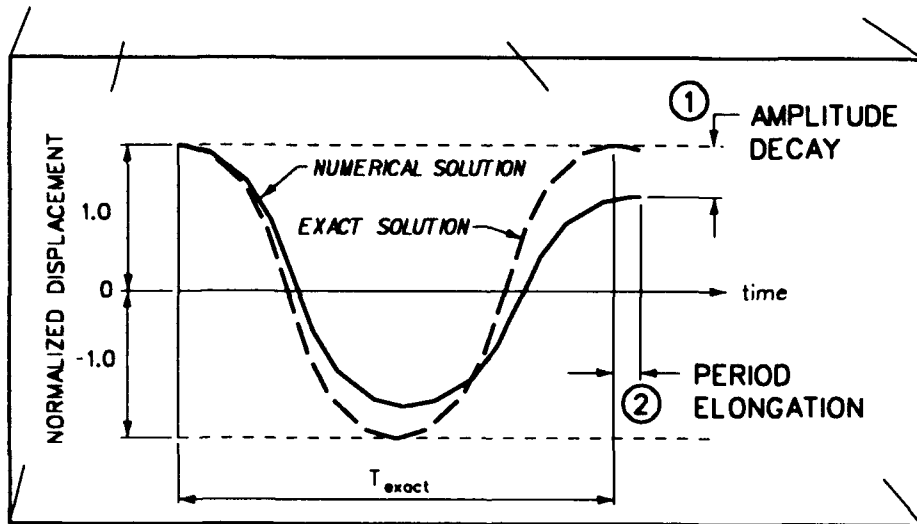
(c) Two errors associated with inaccurate numerical
solution

Figure 14.   Example of inaccurate response for an undamped
SDOF system in free vibration

34

the errors of an algorithm (i.e. amplitude decay and period elongation) as a function of the time step size Δt used in the calculation and the natural period T of the numerical model. Examples of these types of error plots for select algorithms are shown in Figure 9.3 of Bathe and Wilson (1976) and in Figures 9.3.2 and 9.3.3 of Hughes (1987). This decision for a complex MDOF semidiscrete finite element model will depend upon the highest (mode) frequency of engineering interest for the structural system (see Chapter 9 of Hughes 1987).

43. This part describes the construction of response spectra which are graphs of the maximum values of acceleration, velocity, and/or displacement response of an infinite series of damped elastic SDOF systems (Figure 10) subjected to an acceleration time history $\ddot{x}_{ground}(t)$. These maximum response values for several levels of damping are plotted against undamped natural period (units of seconds) or plotted against undamped natural cyclic frequency of vibration (units of hertz or cycles/sec).

Ground Acceleration Time History

44. Figure 15 earthquake accelerogram will be used as the ground motion in this example. It is the South 00 degrees East (S00E) horizontal component recorded at the El Centro site in Southern California during the Imperial Valley Earthquake of 18 May 1940 (Richter magnitude = 6.7). The recording station is founded on alluvium. The peak ground acceleration is equal to 341.7 cm/sec/sec (0.35 g) at 2.12 sec into ground shaking. The ground velocity and displacement curves were obtained by double integration of the acceleration time history. The peak velocity and peak displacement of the ground occur at 2.19 sec and 8.7 sec, respectively. It is typical for the three peak values to occur at different times during earthquake shaking.

45. Figure 15 accelerogram started out as an analog trace recorded by a strong motion accelerograph. The acceleration trace ·;as digitized and fil-tered in order to control errors, with baseline and transducer corrections applied to the accelerogram. Further details regarding the development of a corrected accelerogram are described in Hudson (1979). The California Insti-tute of Technology (Cal Tech) has a strong motion data program that develops corrected accelerograms defined at 0.02 sec time intervals. The corrected accelerograms are often referred to as the Cal Tech Volume II corrected accelerograms.

Response Spectrum

46. A response spectrum is a graphical relationship of maximum values of acceleration, velocity, and/or displacement response of an infinite series of linear SDOF systems with constant damping ratio β shaken by the same

IMPERIAL VALLEY EARTHQUAKE   MAY 18, 1940 - 2037 PST

IIA001 40.001.0   EL CENTRO SITE IMPERIAL VALLEY IRRIGATION DISTRICT   COMP S00E
O PEAK VALUES : ACCEL = 341.7 CM/SEC/SEL   VELOCITY = 33.4 CM/SEC   DISPL = 10.9 CM
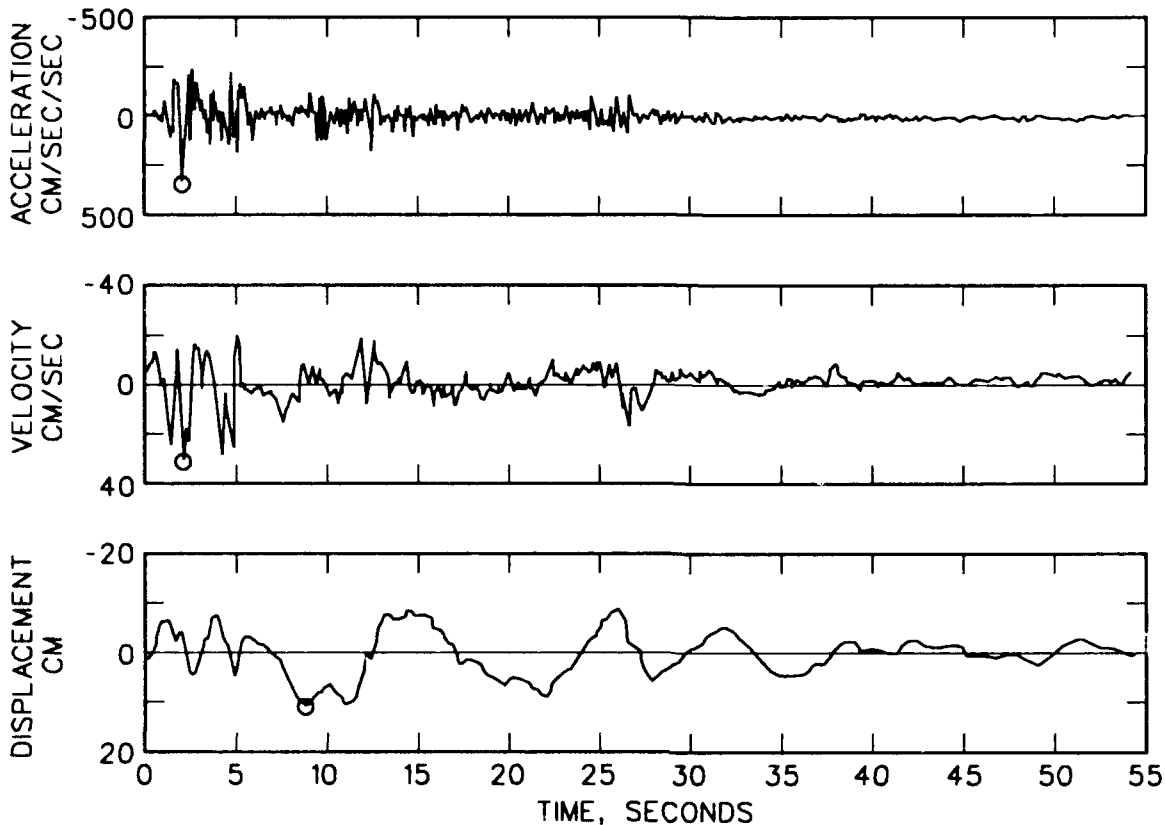
Figure 15. Ground acceleration and integrated ground velocity and
displacement time histories, 1940 El Centro S00E component, from
Hudson (1979)

Figure 15 acceleration time history in this example. Each Figure 10 SDOF sys-
tem is distinguished by the value selected for its undamped natural period of
vibration T (Equation 13) or equivalently, its undamped natural cyclic fre-
quency of vibration f (Equation 14). In the following example β is
arbitrarily set equal to 0.02.

Peak Response Values for Each SDOF System

47. The construction of the response spectrum plots a succession of
SDOF systems with fundamental periods T ranging from near zero to values of
several seconds. For each SDOF system of value T, the dynamic response is
computed using one of the numerical procedures listed in Table 1. The dynamic
response of Figure 10 SDOF system is expressed in terms of either the relative

37

response or the total response of the SDOF system. Response Spectrum values are the maximum response values for each of the five types of SDOF responses for a system of period T and damping β, as described in Table 2. The value assigned to each of the five dynamic response terms for a SDOF system is the peak response value computed during earthquake shaking.

Relative Displacement Response Spectrum

48. The relative displacement response spectrum, S_D or SD, for Figure 15 ground motion is shown in Figure 16, computed for T ranging in value from 0 sec to 3 sec and using $\beta = 0.02$. This figure displays the maximum absolute relative displacement value, $| x(t) |_{max}$, for each of the SDOF systems analyzed, as illustrated by the three plots showing the relative displacement time histories x(t) that were computed using a numerical procedure for the SDOF systems having T equal to 0.5 sec, 1.0 sec, and 2.0 sec, respectively.

$$S_D = | x(t) |_{max} \tag{31}$$

The S_D values for the three SDOF systems are listed in Table 3.

49. A characteristic of relative displacement response spectra is the absence of relative movement between the SDOF system and the ground during earthquake shaking for approximately zero values of T (Figure 16). This is due to the fact that the spring stiffness of a short period, high frequency, SDOF system (refer to the equation for T in Table 2) is so large that it neither stretches nor compresses during ground shaking. At the other extreme, as the value of the spring stiffness is softened (k → 0) and the value for T is greater than 20 sec, the value for S_D approaches the maximum ground displacement (not shown in Figure 16).

Spectral Pseudo-Velocity

50. The spectral pseudo-velocity, S_V or PSV, of the ground motion $\ddot{x}_{ground}(t)$ is computed using

$$S_V = \omega S_D = \frac{2\pi}{T} S_D \tag{32}$$

Table 2

Definition of Earthquake Response Spectrum Terms

Symbols	Definition	Description
S_D – SD	$\|\ x(t)\ \|_{max}$	Relative displacement response spectrum or spectral displacement
SV	$\|\ \dot{x}(t)\ \|_{max}$	Relative velocity response spectrum
SA	$\|\ \ddot{x}_{total}(t)\ \|_{max}$	Absolute acceleration response spectrum
S_v – PSV	$\omega\ S_D - \dfrac{2\pi}{T}\ S_D$	Spectral pseudo-velocity
S_A – PSA	$\omega^2\ S_D - \dfrac{4\pi^2}{T^2}\ S_D$	Spectral pseudo-acceleration

ω is the circular frequency of vibration of the undamped SDOF system in units of radians per second.

$$\omega = \sqrt{\frac{k}{m}}$$

T is the natural (or fundamental) period of vibration of the undamped SDOF system in units of seconds.

$$T = 2\pi\sqrt{\frac{m}{k}}$$

for each of the SDOF systems analyzed. S_v is distinguished from the relative velocity response spectrum SV, to be described in a subsequent paragraph. S_v for Figure 15 ground motion shown in Figure 17b was computed using Equation 32 for each T ranging in value from 0 to 3 sec (at closely spaced intervals) in the figure (β – 0.02). For example, with S_D – 2.48 inches for the T – 0.5 sec (ω – 12.566 radians/sec) SDOF system, S_v = 31.16 inch/sec by Equation 32, and identified in Figure 17b. The values of S_v for the T – 1.0 sec and T – 2.0 sec SDOF systems are listed in Table 3.

51. The term S_v is related to the maximum strain energy stored within the linear spring portion of the SDOF system when the damping force is neglected,
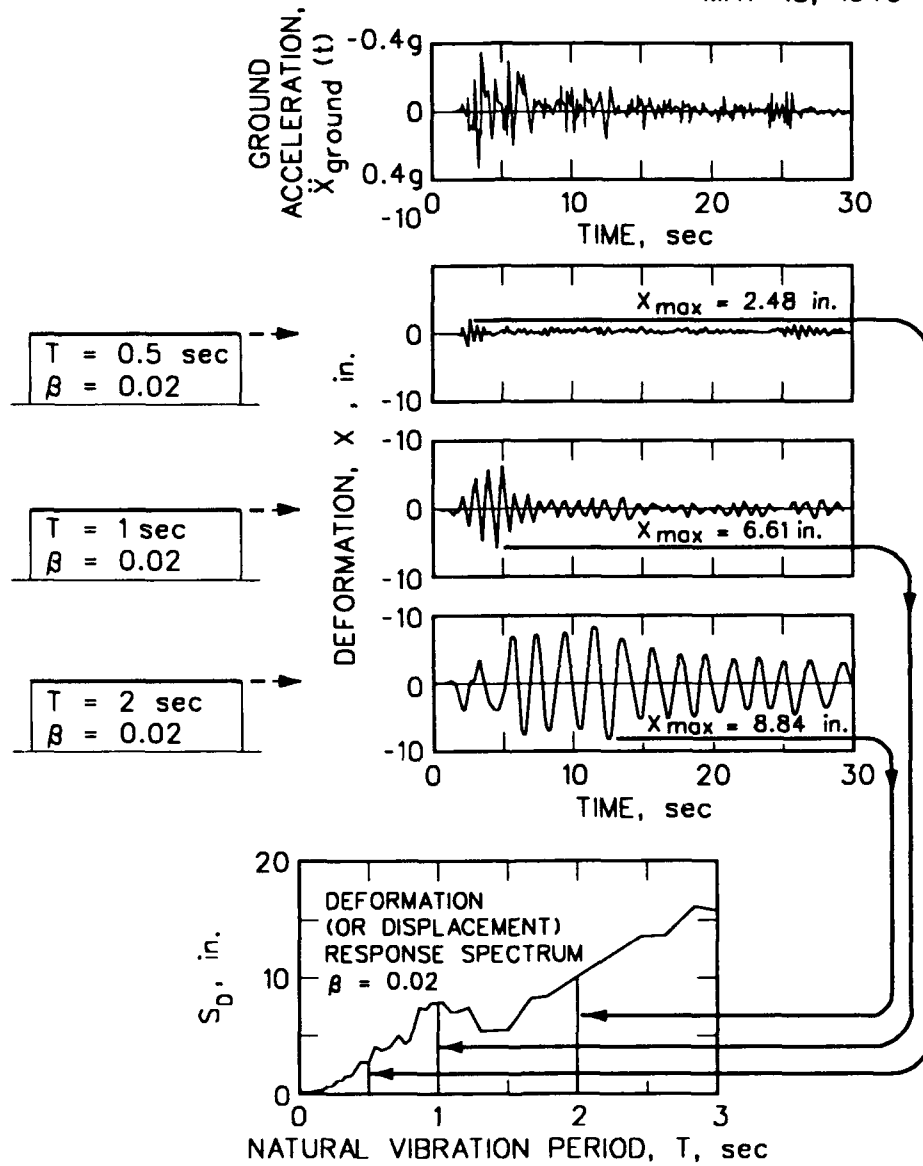
Figure 16. Computation of displacement response spectrum
β = 0.02, 1940 El Centro S00E component, from
Chopra (1981)

Title: Table 3, Response Spectral Values for Three SDOF Systems with β = 0.02, 1940 El Centro S00E Component

Table with columns: T (sec), ω (radians/sec), S_D (inch), S_V (inch/sec), S_A (inch/sec/sec), (g)

Table 3

Response Spectral Values for Three SDOF Systems
with $\beta = 0.02$, 1940 El Centro S00E Component

T (sec)	ω (radians/sec)	S_D (inch)	S_V (inch/sec)	S_A (inch/sec/sec)	(g)
0.5	12.566	2.48	31.16	391.62	1.014
1.0	6.283	6.61	41.53	260.95	0.676
2.0	3.142	8.84	27.77	87.25	0.226

ω is the circular frequency of vibration of the undamped SDOF system

$$\omega = \frac{2\pi}{T}$$

where T is the natural (or fundamental) period of vibration of the undamped SDOF system.

The spectral pseudo-velocity, $S_V = \omega\, S_D$

The spectral pseudo-acceleration, $S_A = \omega^2\, S_D$

1 g - 386.08858 inch/sec/sec

$$Energy_{max} = \frac{1}{2}\, k\, S_D^2 = \frac{1}{2}\, m\, S_V^2 \tag{33}$$

Relative Velocity Response Spectrum

52. The relative velocity response spectrum SV is the maximum absolute value of the computed relative velocity time history (from step 1 of Figure 10) for the SDOF system.

$$SV = |\,\dot{x}(t)\,|_{max} \tag{34}$$

As the value of the period T approaches infinity (i.e. long period SDOF systems), the value for SV approaches the maximum ground velocity $|\,\dot{x}_{ground}(t)\,|_{max}$.

S_D = 2.48 in.

S_V = 31.16 in. /sec

S_A = 1.014 g

T = 0.5 sec

NATURAL VIBRATION PERIOD, T, sec
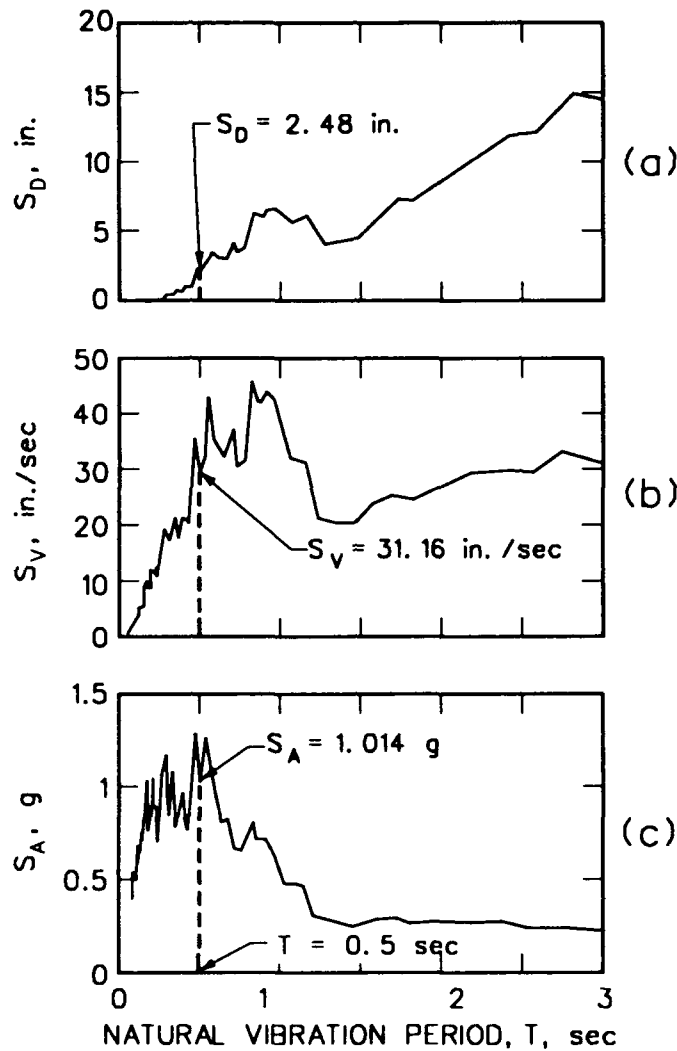
Figure 17. Displacement, pseudo-velocity
pseudo-acceleration linear response
spectra plots, β - 0.02, 1940 El Centro
S00E component, from Chopra (1981)

Comparison of S_V and SV Values

53. The pseudo-velocity value S_V for a SDOF system of period T is not
equivalent to the relative velocity value SV, as shown using expressions
derived for S_V and SV in Appendix A and expressed in terms of the Duhamel's
Integral. However, for a limited range of periods, the value for S_V is an
approximation to the SV value, with the differences between the values
increasing with increasing values for period T. Specifically, for short
periods (i.e. high frequencies) the values for S_V are nearly the same as the

42

values for SV. For long periods or low frequencies, the differences in the
values for S_V and SV can be significant.

Spectral Pseudo-Acceleration

54. The spectral pseudo-acceleration, S_A or PSA, of the ground motion
$\ddot{x}_{ground}(t)$ is computed using either

$$S_A = \omega \; S_V = \frac{2\pi}{T} \; S_V \tag{35}$$

or

$$S_A = \omega^2 \; S_D = \frac{4\pi^2}{T^2} \; S_D \tag{36}$$

for each of the SDOF systems analyzed. S_A is distinguished from the absolute
acceleration response spectrum SA to be described in a subsequent paragraph.
S_A for Figure 15 ground motion, shown in Figure 17c was computed using either
Equation 35 or Equation 36 for each T ranging in value from 0 to 3 sec in the
figure (β - 0.02%). For example, with S_D - 2.48 inches for the T - 0.5 sec
(ω - 12.566 radians/sec) SDOF system, S_A - 391.62 inch/sec/sec (1.014 g) by
Equation 36 and identified in Figure 17c. The values of S_A for the T -
1.0 sec and T - 2.0 sec SDOF systems are listed in Table 3. The force com-
puted as the product of the mass m times S_A is a good approximation to the
maximum force in the spring.

Absolute Acceleration Response Spectrum

55. The absolute acceleration response spectrum SA is the maximum abso-
lute value of the sum of the computed relative acceleration time history for
the SDOF system plus the ground acceleration time history (from step 2 in
Figure 10).

$$SA = | \ddot{x}_{total}(t) |_{max} = | \ddot{x}_{ground}(t) + \ddot{x}(t) |_{max} \tag{37}$$

Comparison of S_A and SA Values

56. The pseudo-acceleration value S_A for a SDOF system of period T is equal to the absolute acceleration value SA when β - 0 (refer to Appendix A). For the low levels of damping common to structural dynamics problems, the values for S_A and SA are nearly equal over the period range of interest.

57. For short period, high frequency, stiff SDOF systems (T < 0.05 sec), the values for S_A and SA are equal to the peak ground acceleration | $\ddot{x}_{ground}(t)$ |$_{max}$, as shown in Figure 18. As the period T approaches infinity (i.e. massive SDOF systems), the values for SA and S_A approach zero (not shown in Figure 18).

Tripartite Response Spectra Plot

58. A tripartite response spectrum plot is a logarithmic plot of the three SDOF response quantities S_D, S_V, and S_A as a function of the undamped fundamental period T in units of seconds (or cyclic frequency f in units of hertz). The tripartite response spectrum plot for Figure 15 ground motion is shown in Figure 19, with the response spectrum values computed for each T ranging in value from 0.04 to 3 sec in the figure (β - 0.02). The plot uses four logarithmic scales: the period T along the abscissa, S_V along the ordinate, S_A along an axis oriented at 45 deg counterclockwise from horizontal, and S_D along an axis oriented at 45 deg clockwise from horizontal. The response quantities S_D - 2.48 inches, S_V - 31.16 inch/sec, and S_A - 1.014 g for the T - 0.5 sec SDOF system identified in Figure 19.

59. Figure 19 tripartite response spectrum plot has the advantage of condensing the information presented using three plots in Figure 17 onto a single plot because of the interrelationships between the three terms (refer to Equations 32, 35, and 36).

60. The tripartite response spectrum plot for the 1940 El Centro ground motion (Figure 15) in Figure 20 shows the response spectrum values for levels of damping, β - 0, 0.02, 0.05, 0.1 and 0.2. This figure illustrates the trend common to all ground motions of increased values for S_D, S_V, and S_A with lower damping levels.

PEAK GROUND ACCELERATION = $\left|\ddot{x}_{ground}(t)\right|_{max}$ = $SA_1(T_1)$ = $S_{A1}(T_1)$

SA and S_A

S_A, SPECTRAL PSEUDO-ACCELERATION

SA, ABSOLUTE ACCELERATION RESPONSE SPECTRUM

SA_2

SA_3

DAMPING

β = CONSTANT

MAX

T_1 = 0

GROUND ACCELERATION $(T_1 = 0$ sec)

MAX

t_1

time

TOTAL ACCELERATION for T_2

t_2

time

T_2

T_3

T
PERIOD
(sec)

MAX

TOTAL ACCELERATION for T_3

t_3

time

$$SA = \left|\ddot{x}_{total}(t)\right|_{max} = \left|\ddot{x}_{ground}(t) + \ddot{x}(t)\right|_{max}$$

$$S_A = \omega^2 S_D$$
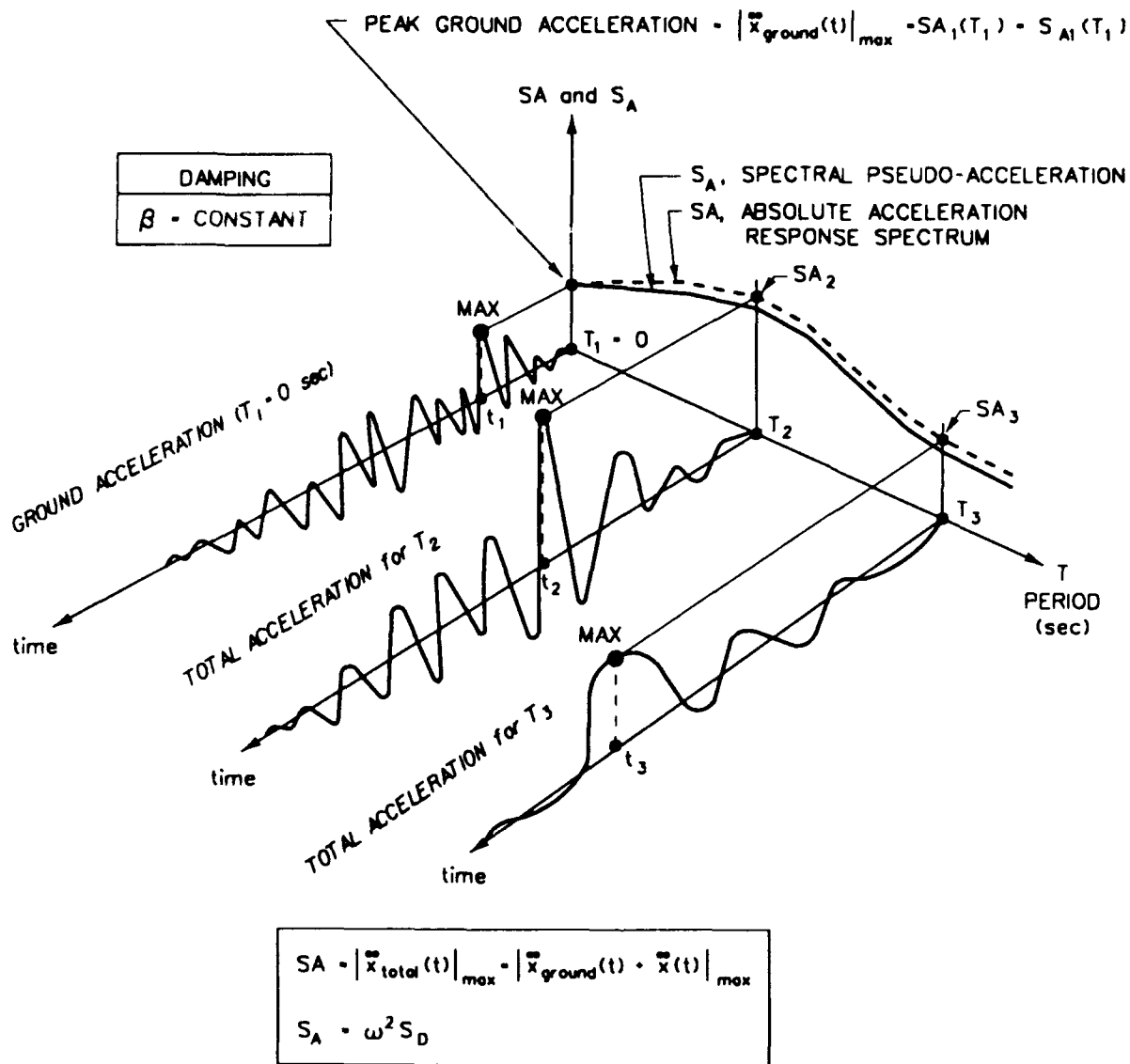
Figure 18.   Pseudo-acceleration and absolute acceleration linear response
spectrum plots

Fundamental Periods at Which the Maximum Values for

S_A, S_V, and S_D are Computed

61.   For the 1940 El Centro ground motion, the largest value of S_A equal
to 1.29 g (1,265 cm/sec/sec), for an SDOF system with T equal to 0.47 sec (f =
2.13 Hz) and β = 0.02 (refer to Figure 17 or Figures 19 and 20).   This value
is 3.7 times larger than the peak acceleration value of 0.35 g (341.7 cm/sec/
sec) of the accelerogram (Figure 15).   The largest value for S_V, equal to
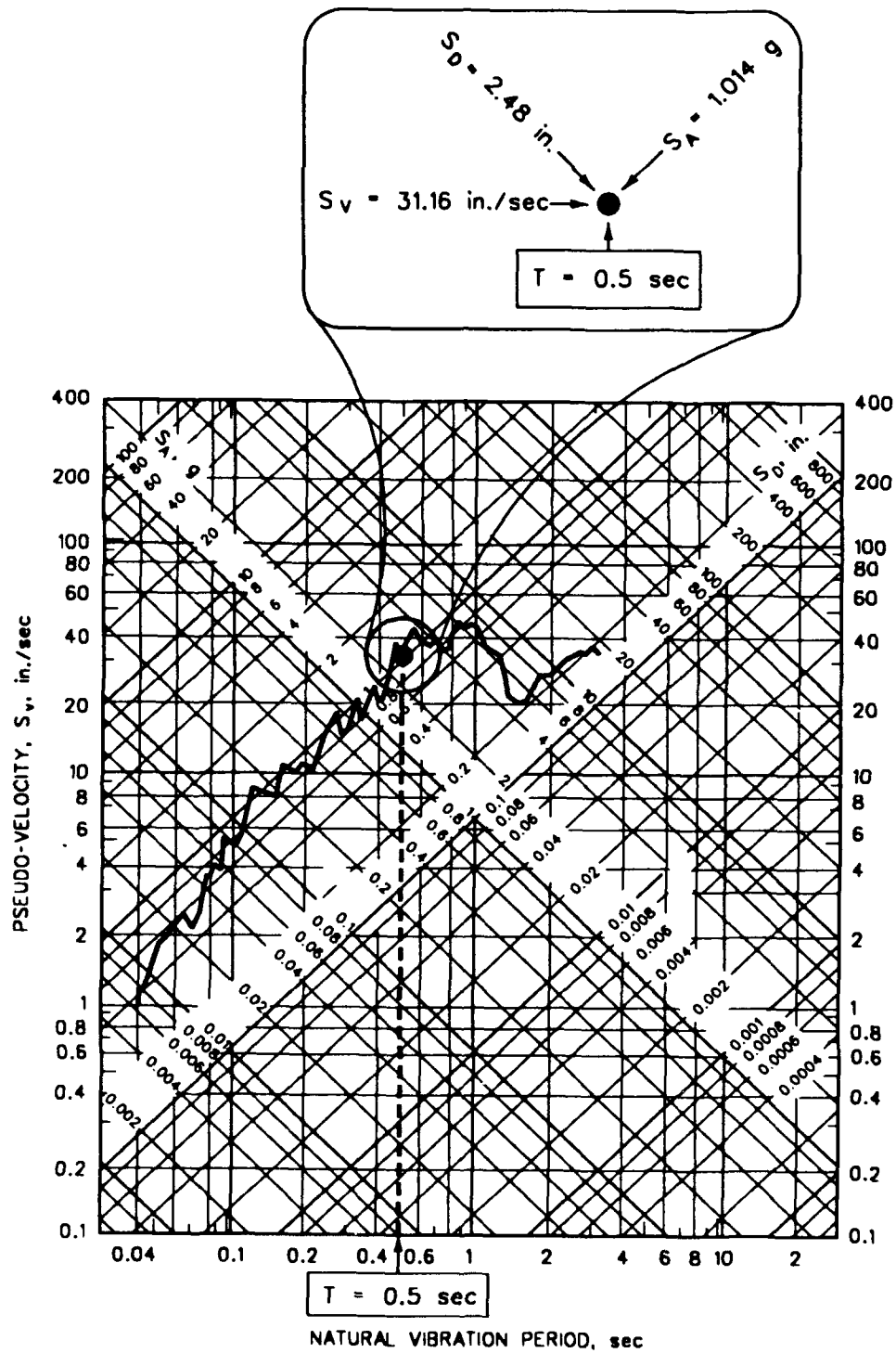
Figure 19.   Tripartite logarithmic plot of response spectrum,
$\beta = 0.02$, 1940 EL Centro S00E component, from Chopra (1981)

46

RESPONSE SPECTRUM

IMPERIAL VALLEY EARTHQUAKE   MAY 18, 1940 - 2037 PST
IIIA001 40.001.0 EL CENTRO SITE IMPERIAL VALLEY IRRIGATION DISTRICT   COMP SOOE
DAMPING VALUES ARE 0, 2, 5, 10, AND 20 PERCENT OF CRITICAL
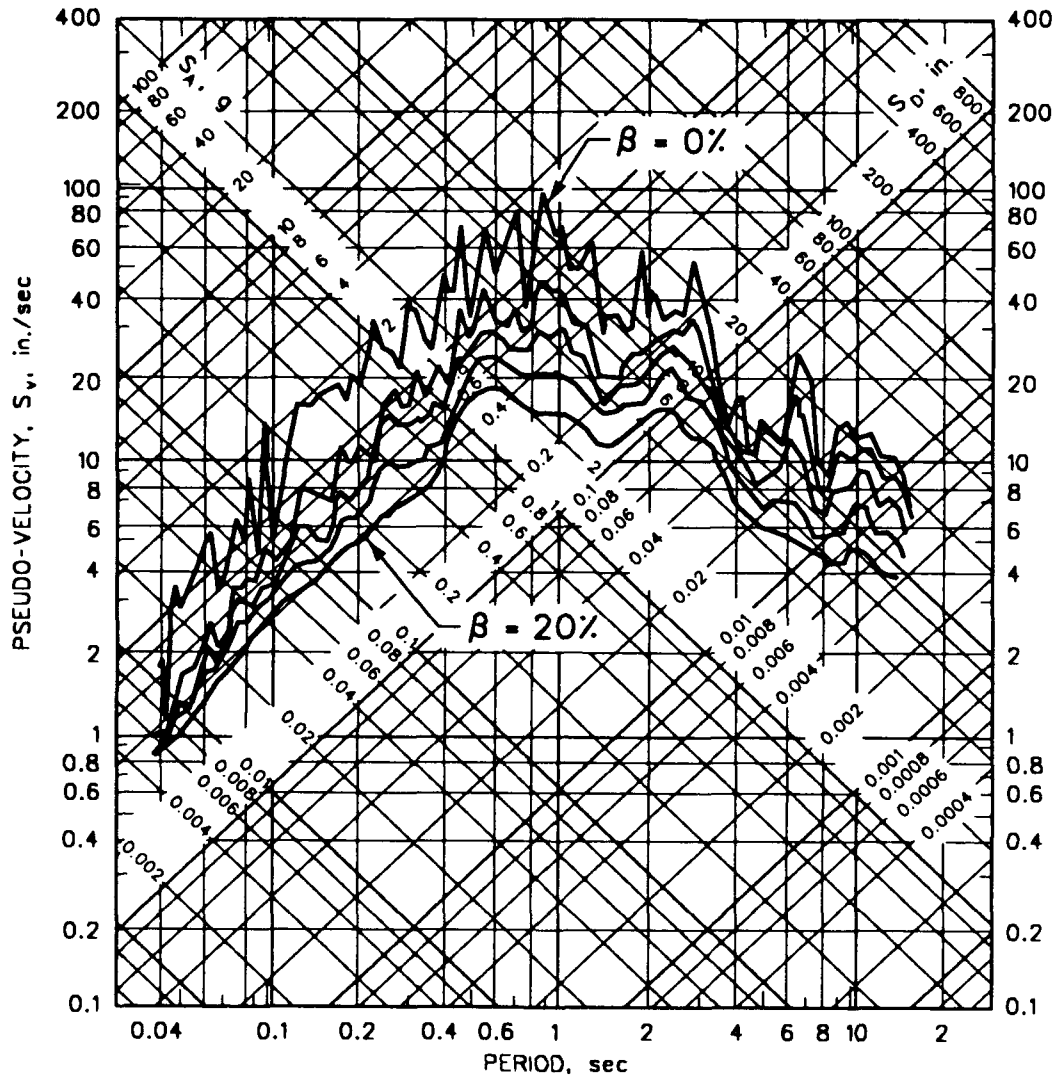
Figure 20.   Tripartite logarithmic plot of response spectrum, $\beta = 0$, 0.02, 0.05, 0.1, and 0.2, 1940 El Centro S00E Component, from Chopra (1981)

45.7 in./sec (18 cm/sec), is computed for a value of T equal to 0.84 sec (f = 1.19 Hz). The largest value for S_D, equal to 18 in. (7.09 cm), is computed for a value of T equal to 10.5 sec (f = 0.095 Hz) (Figure 20). The order of increasing T values (seconds) with the peak values of S_A, S_V, and S_D is typical of response spectra for ground motions. The order of spectral values is reversed when the SDOF system is described in terms of increasing values of cyclic frequency f (Hz) (Equation 14).

47

Frequency Regions of the Tripartite Response Spectra

62. Although quite irregular with local peaks and spikes, the 1940 El Centro earthquake motion tripartite response spectrum has the general shape of a trapezoid or tent (refer to Figure 20). This general shape implies three distinct regions with regards to the frequency content of the 1940 El Centro earthquake motion.

63. Within the short period range of $1/8$ sec $< T < 1/2$ sec or equivalently, the high frequency range of 2 Hz $< f <$ 8 Hz, S_A is nearly constant (an average value of 0.95 g (931.6 cm/sec/sec) with a variation equal to $\pm$ 25%), as compared to the variation in S_V and S_D values (Figure 19).

64. There are two distinct subregions within the intermediate period range of the 1940 El Centro motion response spectra shown in Figure 19. The first subregion is within the period range of $1/2$ sec $< T < 1$ sec (1 Hz $< f <$ 2 Hz), with S_V a nearly constant 38 in/sec (15 cm/sec) value ($\pm$ 20%), as compared to the variation in S_A and S_D values. Between 1 sec $< T <$ 3 sec (or 0.33 Hz $< f <$ 1 Hz), S_V is nearly a constant 28 in./sec (11 cm/sec) value ($\pm$ 25%).

65. The long period range, T greater than 3 sec (the low frequency range of $f <$ 0.33 Hz), S_D averages 13 in (5.1 cm) for $\beta = 0.02$, with a variation equal to $\pm$ 40% (Figure 20). For this accelerogram, the variation in the average value of S_D is greater than the variations in the S_A and S_V values for the short and intermediate period ranges, respectively.

Design Response Spectra

66. The previously described trends in the spectral content with frequency of earthquake accelerograms were recognized in the 1970's by numerous earthquake engineers and seismologists. Statistical analyses of response spectra of earthquake motions were conducted by several groups with the objectives of identifying the factors affecting the response spectra for earthquake motions, characterizing shape or the frequency content of the earthquake spectrum for the category under study and developing smooth, broad band spectrum for use in the design of structures for earthquake loadings. A broad band spectrum ensures that sufficient seismic energy is delivered to all frequencies.

67. The results of some of the early ground motion studies are summarized in Seed, Ugas, and Lysmer (1976), Mohraz (1976), and Newmark and Hall (1982). Their results show that the spectra frequency content of the recorded accelerograms are dependent upon the earthquake magnitude, distance from causative fault to site, the type of substratum on which the recording station is founded (i.e., rock, shallow alluvium, or deep alluvium), and the tectonic environment. Using standard regression techniques for selected ground motion categories, (smooth) trends in the variation in spectral content with frequency were quantitatively identified, as well as their variation about their median values, expressed in terms of a standard deviation.

Newmark and Hall Design Response Spectrum

68. The Newmark and Hall (1982) design response spectrum exemplifies the important features common to current procedures used to characterize the spectral content of earthquake motions. A Newmark and Hall tripartite design response spectrum for a moderate earthquake at a competent soil site corresponds to the solid line shown in Figure 21 for $\beta = 0.05$. The peak ground acceleration, peak ground velocity, and peak ground displacement used in this example and included for reference in this figure (dashed line), are 0.5 g (490.3 cm/sec/sec), 61 cm/sec, and 45 cm, respectively. The spectral values are plotted as a function of the frequency f (Hz), rather than period T as Figures 19 and 20. The Newmark and Hall design response spectrum is a smooth, broad band spectrum composed of three distinct regions of constant, limiting spectral values for S_A, S_V, and S_D, as identified in the figure. These spectral amplitude values correspond to one standard deviation above the median spectral values (84.1 % cumulative probability). Mean spectral values are presented in the Newmark and Hall (1982) publication as well. A smooth, broad band spectrum ensures that sufficient seismic energy is delivered to all frequencies in a dynamic analysis of a MDOF semidiscrete structural model. For details regarding the construction of the Newmark and Hall design response spectrum, consult their 1982 EERI monograph.

Response Spectrum in the Dynamic Analysis of MDOF Structural Models

69. The response spectrum is used to represent the seismic loading in the dynamic analysis of MDOF semidiscrete structural models. For details
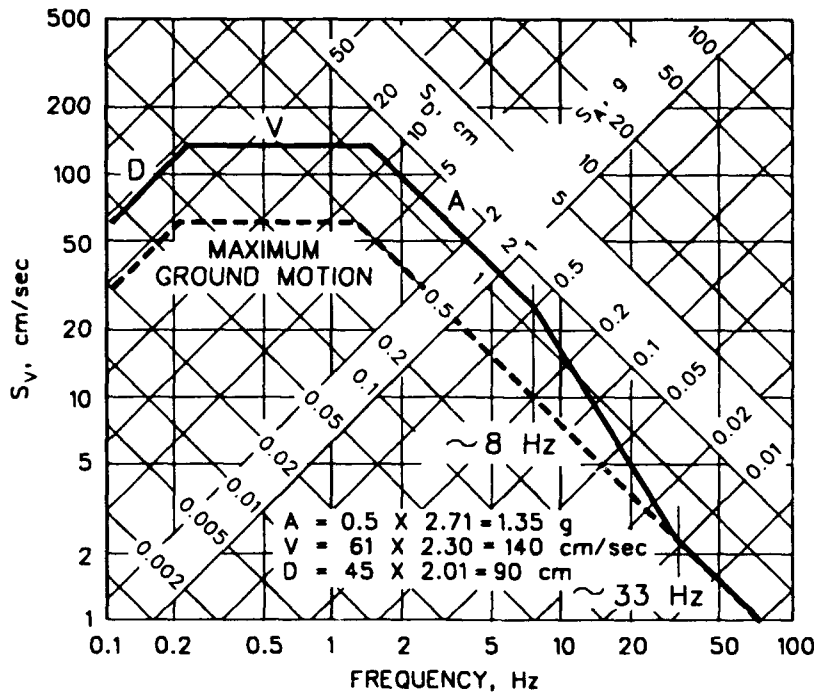
Figure 21. Newmark and Hall elastic design response
spectrum, from Newmark and Hall (1982)

regarding its application in structural dynamic problems, the reader is
referred to textbooks such as Clough and Penzien (1975), Chopra (1981), or Paz
(1985).

REFERENCES

Bathe, K. J. 1982. <u>Finite Element Procedures in Engineering Analysis,</u> Prentice-Hall, Englewood Cliffs, NJ, 735 p.

Bathe, K. J. and Wilson, E. W. 1976. <u>Numerical Methods In Finite Element Analysis,</u> Prentice-Hall, Englewood Cliffs, NJ, 735 p.

Chopra, A. 1981. <u>Dynamics of Structures, A Primer,</u> Earthquake Engineering Research Institute, Berkeley, CA, 126 p.

Clough, R. W. and Penzien, J. 1975. <u>Dynamics of Structures,</u> McGraw-Hill, New York, NY, 634 p.

Dokainish, M. A. and Subbaraj, K. 1989. "A Survey of Direct Time-Integration Methods in Computational Structural Dynamics-II. Implicit Methods," Computers and Structures (printed in Great Britain), Vol. 32, No. 6, pp. 1387-1401.

Hudson, D. E. 1979. <u>Reading and Interpreting Strong Motion Accelerograms,</u> Earthquake Engineering Research Institute, Berkeley, CA, 112 p.

Hughes, T. J. R. 1987. <u>The Finite Element Method, Linear Static and Dynamic Finite Element Analysis,</u> Prentice-Hall, Englewood Cliffs, NJ, 803 p.

Hughes, T. J. R. and Belytshko, T. 1983 (Dec.). "A Precis of Developments in Computational Methods for Transient Analysis," Transactions of the ASME Journal of Applied Mechanics, Vol. 50, pp. 1033-1041.

Kreyszig, E. 1972. <u>Advanced Engineering Mathematics,</u> John Wiley and Sons, Inc, New York, NY, 866 p.

Mohraz, B. 1976. "A Study of Earthquake Response Spectra for Different Geological Conditions," Bulletin of the Seismological Society of America, Vol. 66, No. 3, pp. 915-935.

Newmark, N. M. and Hall, W. J. 1982. <u>Earthquake Spectra and Design,</u> Earthquake Engineering Research Institute, Berkeley, CA, 103 p.

Newmark, N. M. and Rosenblueth, E. 1971. <u>Fundamentals of Earthquake Engineering,</u> Prentice-Hall, Inc., Englewood Cliffs, NJ, 640 p.

Paz, M. 1985. <u>Structural Dynamics, Theory and Computation,</u> Van Nostrand Reinhold Company, Inc., New York, NY, 561 p.

Seed, H. B., Ugas, C., and Lysmer, J. 1976. "Site Dependent Spectra for Earthquake-Resistant Design," Bulletin of the Seismological Society of America, Vol. 66, No. 1, pp. 221-244.

APPENDIX A: SOLUTIONS FOR SPECTRAL TERMS BASED UPON DUHAMEL'S INTEGRAL SOLUTION FOR RELATIVE DISPLACEMENT

1. This appendix describes the derivation of relationships for each of the five response spectrum terms S_D, S_V, SV, S_A, and SA (Table 2), expressed in terms of Duhamel's integral. The resulting relationships show that the terms S_V and SV are not equivalent, while the terms S_A and SA are equivalent only if $\beta = 0$.

Duhamel's Integral Solution for Relative Displacement

2. The relative displacement of the SDOF system was described in Part IV involving Duhamel's integral. The derivation of x(t) (Equation 22) involved the representation of the load time history $P(t) = - m\ddot{x}_{ground}$ as a series of loadings $P(\tau) = - m\ddot{x}_{ground}$ applied to the SDOF system for short duration time intervals $d\tau$. The resulting relationship for a damped SDOF system is given as

$$x(t) = - \frac{1}{\omega_D} \int_0^t \ddot{x}_{ground}(\tau) \ e^{-\beta\omega(t-\tau)} \sin [\omega_D(t - \tau)] \ d\tau \tag{A1}$$

where

ω_D = the damped angular frequency of vibration (Equation 16)

ω = the undamped angular frequency of vibration (Equation 11)

β = the fraction of critical damping (Equation 12).

Relative Displacement Response Spectrum S_D
Expressed in Terms of Duhamel's Integral

3. The relative displacement response spectrum S_D is equal to the maximum absolute relative displacement value $| \ x(t) \ |_{max}$ (Equation 25) for a damped SDOF system of period T. Introducing Equation A1 for the relative displacement x(t), S_D becomes

$$S_D = \left| - \frac{1}{\omega_D} \int_0^t \ddot{x}_{ground}(\tau) \ e^{-\beta\omega(t-\tau)} \sin [\omega_D(t - \tau)] \ d\tau \right|_{max} \tag{A2}$$

A1

4. S_V may be expressed in terms of Duhamel's integral by introducing the Duhamel's integral solution for S_D into Equation 26, resulting in the relationship for S_V is given by

$$S_V = \left| -\frac{\omega}{\omega_D} \int_0^t \ddot{x}_{ground}(\tau)\ e^{-\beta\omega(t-\tau)} \sin\ [\omega_D(t-\tau)]\ d\tau \right|_{max} \qquad (A3)$$

For an undamped SDOF system ($\beta = 0$), this expression simplifies to

$$S_V = \left| -\int_0^t \ddot{x}_{ground}(\tau)\ \sin\ [\omega(t-\tau)]\ d\tau \right|_{max} \qquad (A4)$$

Relative Velocity Response Spectrum SV Expressed in Terms of Duhamel's Integral

5. The relative velocity response spectrum SV is equal to the maximum absolute relative velocity value $|\ \dot{x}(t)\ |_{max}$ (Equation 28) for a damped SDOF system of period T. Differentiating Duhamel's integral solution for relative displacement (Equation A1) with respect to time results in an expression for $\dot{x}(t)$, with SV equal to the maximum absolute value of the resulting expression.

$$SV = \left| \begin{array}{l} -\int_0^t \ddot{x}_{ground}(\tau)\ e^{-\beta\omega(t-\tau)} \cos\ [\omega_D(t-\tau)]\ d\tau \\[2mm] +\dfrac{\beta}{\sqrt{1-\beta^2}} \int_0^t \ddot{x}_{ground}(\tau)\ e^{-\beta\omega(t-\tau)} \sin\ [\omega_D(t-\tau)]\ d\tau \end{array} \right|_{max} \qquad (A5)$$

Refer to page 62 of Hudson (1979) or section 1.5 of Newmark and Rosenbluth (1971)*. For an undamped SDOF system ($\beta = 0$) Equation A5 becomes

$$SV = \left| -\int_0^t \ddot{x}_{ground}(\tau)\ \cos\ [\omega(t-\tau)]\ d\tau \right|_{max} \qquad (A6)$$

---

* References cited in this appendix are included in the References at the end of the main text.

Comparison of Spectral Pseudo-Velocity and Relative Velocity
Response Spectrum Relationships

6. Comparison of the expressions for S_V (Equation A3) and SV (Equation A5) in the previous two paragraphs demonstrates the difference between the two terms. The simplified relationships for an undamped SDOF system ($\beta = 0$) shows the terms for S_V (Equation A4) and SV (Equation A6) differ by the trigonometric function used within Duhamel's integral.

Spectral Pseudo-Acceleration S_A Expressed in
Terms of Duhamel's Integral

7. S_A may be expressed in terms of Duhamel's integral by introducing the Duhamel's integral solution for S_D into Equation 30, resulting in the relationship for S_A given by

$$S_A = \left| - \frac{\omega^2}{\omega_D} \int_0^t \ddot{x}_{ground}(\tau) \ e^{-\beta\omega(t-\tau)} \sin\left[\omega_D(t-\tau)\right] \ d\tau \right|_{max} \tag{A7}$$

For an undamped SDOF system ($\beta = 0$), this expression simplifies to

$$S_A = \left| - \omega \int_0^t \ddot{x}_{ground}(\tau) \sin\left[\omega(t-\tau)\right] \ d\tau \right|_{max} \tag{A8}$$

Absolute Acceleration Response Spectrum in
Terms of Duhamel's Integral

8. The absolute acceleration response spectrum SA is the maximum absolute value of the sum of the computed relative acceleration time history for the SDOF system plus the ground acceleration time history.

$$SA = \left| \ddot{x}_{total}(t) \right|_{max} = \left| \ddot{x}_{ground}(t) + \ddot{x}(t) \right|_{max} \tag{A9}$$

To introduce Duhamel's integral solution for relative displacement into this relationship, $\ddot{x}_{total}(t)$ is expressed in terms of the relative velocity and

relative displacement of the SDOF system. Rearranging the dynamic equilibrium Equation 21 and introducing

$$\ddot{x}_{total} = \ddot{x}_{ground} + \ddot{x} \tag{A10}$$

results in the relationship

$$\ddot{x}_{total} = -2\beta\omega\dot{x} - \omega^2 x \tag{A11}$$

Introducing Equation A1 and the term within the absolute value in Equation A5 into Equation A11, results in the relationship

$$SA = \left| \begin{array}{c} 2\omega\beta \int_0^t \ddot{x}_{ground}(\tau)\ e^{-\beta\omega(t-\tau)} \cos\ [\omega_D(t-\tau)]\ d\tau \\[2ex] + \dfrac{\omega(1-2\beta^2)}{\sqrt{1-\beta^2}} \int_0^t \ddot{x}_{ground}(\tau)\ e^{-\beta\omega(t-\tau)} \sin\ [\omega_D(t-\tau)]\ d\tau \end{array} \right|_{max} \tag{A12}$$

Refer to page 63 of Hudson (1979) or section 1.5 of Newmark and Rosenbluth (1971). For an undamped SDOF system ($\beta = 0$) Equation A12 becomes

$$SA = \left| -\omega \int_0^t \ddot{x}_{ground}(\tau) \sin\ [\omega(t-\tau)]\ d\tau \right|_{max} \tag{A13}$$

Comparison of Spectral Pseudo-Acceleration and Absolute Acceleration Response Spectrum Relationships

9. Comparison of the expressions for S_A (Equation A7) and SA (Equation A12) in the previous two paragraphs demonstrates the difference between the two terms. However, the simplified relationships for an undamped SDOF system ($\beta = 0$) for S_A (Equation A8) and SA (Equation A13) are the same.

WATERWAYS EXPERIMENT STATION REPORTS
PUBLISHED UNDER THE COMPUTER-AIDED
STRUCTURAL ENGINEERING (CASE) PROJECT

	Title	Date
Technical Report K-78-1	List of Computer Programs for Computer-Aided Structural Engineering	Feb 1978
Instruction Report O-79-2	User's Guide: Computer Program with Interactive Graphics for Analysis of Plane Frame Structures (CFRAME)	Mar 1979
Technical Report K-80-1	Survey of Bridge-Oriented Design Software	Jan 1980
Technical Report K-80-2	Evaluation of Computer Programs for the Design/Analysis of Highway and Railway Bridges	Jan 1980
Instruction Report K-80-1	User's Guide: Computer Program for Design/Review of Curvilinear Conduits/Culverts (CURCON)	Feb 1980
Instruction Report K-80-3	A Three-Dimensional Finite Element Data Edit Program	Mar 1980
Instruction Report K-80-4	A Three-Dimensional Stability Analysis/Design Program (3DSAD)	
	Report 1: General Geometry Module	Jun 1980
	Report 3: General Analysis Module (CGAM)	Jun 1982
	Report 4: Special-Purpose Modules for Dams (CDAMS)	Aug 1983
Instruction Report K-80-6	Basic User's Guide: Computer Program for Design and Analysis of Inverted-T Retaining Walls and Floodwalls (TWDA)	Dec 1980
Instruction Report K-80-7	User's Reference Manual: Computer Program for Design and Analysis of Inverted-T Retaining Walls and Floodwalls (TWDA)	Dec 1980
Technical Report K-80-4	Documentation of Finite Element Analyses	
	Report 1: Longview Outlet Works Conduit	Dec 1980
	Report 2: Anchored Wall Monolith, Bay Springs Lock	Dec 1980
Technical Report K-80-5	Basic Pile Group Behavior	Dec 1980
Instruction Report K-81-2	User's Guide: Computer Program for Design and Analysis of Sheet Pile Walls by Classical Methods (CSHTWAL)	
	Report 1: Computational Processes	Feb 1981
	Report 2: Interactive Graphics Options	Mar 1981
Instruction Report K-81-3	Validation Report: Computer Program for Design and Analysis of Inverted-T Retaining Walls and Floodwalls (TWDA)	Feb 1981
Instruction Report K-81-4	User's Guide: Computer Program for Design and Analysis of Cast-in-Place Tunnel Linings (NEWTUN)	Mar 1981
Instruction Report K-81-6	User's Guide: Computer Program for Optimum Nonlinear Dynamic Design of Reinforced Concrete Slabs Under Blast Loading (CBARCS)	Mar 1981
Instruction Report K-81-7	User's Guide: Computer Program for Design or Investigation of Orthogonal Culverts (CORTCUL)	Mar 1981
Instruction Report K-81-9	User's Guide: Computer Program for Three-Dimensional Analysis of Building Systems (CTABS80)	Aug 1981
Technical Report K-81-2	Theoretical Basis for CTABS80: A Computer Program for Three-Dimensional Analysis of Building Systems	Sep 1981
Instruction Report K-82-6	User's Guide: Computer Program for Analysis of Beam-Column Structures with Nonlinear Supports (CBEAMC)	Jun 1982

(Continued)

WATERWAYS EXPERIMENT STATION REPORTS
PUBLISHED UNDER THE COMPUTER-AIDED
STRUCTURAL ENGINEERING (CASE) PROJECT

(Continued)

	Title	Date
Instruction Report K-82-7	User's Guide: Computer Program for Bearing Capacity Analysis of Shallow Foundations (CBEAR)	Jun 1982
Instruction Report K-83-1	User's Guide: Computer Program with Interactive Graphics for Analysis of Plane Frame Structures (CFRAME)	Jan 1983
Instruction Report K-83-2	User's Guide: Computer Program for Generation of Engineering Geometry (SKETCH)	Jun 1983
Instruction Report K-83-5	User's Guide: Computer Program to Calculate Shear, Moment, and Thrust (CSMT) from Stress Results of a Two-Dimensional Finite Element Analysis	Jul 1983
Technical Report K-83-1	Basic Pile Group Behavior	Sep 1983
Technical Report K-83-3	Reference Manual: Computer Graphics Program for Generation of Engineering Geometry (SKETCH)	Sep 1983
Technical Report K-83-4	Case Study of Six Major General-Purpose Finite Element Programs	Oct 1983
Instruction Report K-84-2	User's Guide: Computer Program for Optimum Dynamic Design of Nonlinear Metal Plates Under Blast Loading (CSDOOR)	Jan 1984
Instruction Report K-84-7	User's Guide: Computer Program for Determining Induced Stresses and Consolidation Settlements (CSETT)	Aug 1984
Instruction Report K-84-8	Seepage Analysis of Confined Flow Problems by the Method of Fragments (CFRAG)	Sep 1984
Instruction Report K-84-11	User's Guide for Computer Program CGFAG, Concrete General Flexure Analysis with Graphics	Sep 1984
Technical Report K-84-3	Computer-Aided Drafting and Design for Corps Structural Engineers	Oct 1984
Technical Report ATC-86-5	Decision Logic Table Formulation of ACI 318-77, Building Code Requirements for Reinforced Concrete for Automated Constraint Processing, Volumes I and II	Jun 1986
Technical Report ITL-87-2	A Case Committee Study of Finite Element Analysis of Concrete Flat Slabs	Jan 1987
Instruction Report ITL-87-1	User's Guide: Computer Program for Two-Dimensional Analysis of U-Frame Structures (CUFRAM)	Apr 1987
Instruction Report ITL-87-2	User's Guide: For Concrete Strength Investigation and Design (CASTR) in Accordance with ACI 318-83	May 1987
Technical Report ITL-87-6	Finite-Element Method Package for Solving Steady-State Seepage Problems	May 1987
Instruction Report ITL-87-3	User's Guide: A Three Dimensional Stability Analysis/Design Program (3DSAD) Module	Jun 1987
	Report 1: Revision 1: General Geometry	Jun 1987
	Report 2: General Loads Module	Sep 1989
	Report 6: Free-Body Module	Sep 1989

(Continued)

	Title	Date
Instruction Report ITL-87-4	User's Guide: 2-D Frame Analysis Link Program (LINK2D)	Jun 1987
Technical Report ITL-87-4	Finite Element Studies of a Horizontally Framed Miter Gate Report 1: Initial and Refined Finite Element Models (Phases A, B, and C), Volumes I and II Report 2: Simplified Frame Model (Phase D) Report 3: Alternate Configuration Miter Gate Finite Element Studies—Open Section Report 4: Alternate Configuration Miter Gate Finite Element Studies—Closed Sections Report 5: Alternate Configuration Miter Gate Finite Element Studies—Additional Closed Sections Report 6: Elastic Buckling of Girders in Horizontally Framed Miter Gates Report 7: Application and Summary	Aug 1987
Instruction Report GL-87-1	User's Guide: UTEXAS2 Slope-Stability Package; Volume I, User's Manual	Aug 1987
Instruction Report ITL-87-5	Sliding Stability of Concrete Structures (CSLIDE)	Oct 1987
Instruction Report ITL-87-6	Criteria Specifications for and Validation of a Computer Program for the Design or Investigation of Horizontally Framed Miter Gates (CMITER)	Dec 1987
Technical Report ITL-87-8	Procedure for Static Analysis of Gravity Dams Using the Finite Element Method – Phase 1a	Jan 1988
Instruction Report ITL-88-1	User's Guide: Computer Program for Analysis of Planar Grid Structures (CGRID)	Feb 1988
Technical Report ITL-88-1	Development of Design Formulas for Ribbed Mat Foundations on Expansive Soils	Apr 1988
Technical Report ITL-88-2	User's Guide: Pile Group Graphics Display (CPGG) Post-processor to CPGA Program	Apr 1988
Instruction Report ITL-88-2	User's Guide for Design and Investigation of Horizontally Framed Miter Gates (CMITER)	Jun 1988
Instruction Report ITL-88-4	User's Guide for Revised Computer Program to Calculate Shear, Moment, and Thrust (CSMT)	Sep 1988
Instruction Report GL-87-1	User's Guide: UTEXAS2 Slope-Stability Package; Volume II, Theory	Feb 1989
Technical Report ITL-89-3	User's Guide: Pile Group Analysis (CPGA) Computer Group	Jul 1989
Technical Report ITL-89-4	CBASIN—Structural Design of Saint Anthony Falls Stilling Basins According to Corps of Engineers Criteria for Hydraulic Structures; Computer Program X0098	Aug 1989

(Continued)

WATERWAYS EXPERIMENT STATION REPORTS PUBLISHED UNDER THE COMPUTER-AIDED STRUCTURAL ENGINEERING (CASE) PROJECT

(Concluded)

	Title	Date
Technical Report ITL-89-5	CCHAN–Structural Design of Rectangular Channels According to Corps of Engineers Criteria for Hydraulic Structures; Computer Program X0097	Aug 1989
Technical Report ITL-89-6	The Response-Spectrum Dynamic Analysis of Gravity Dams Using the Finite Element Method; Phase II	Aug 1989
Contract Report ITL-89-1	State of the Art on Expert Systems Applications in Design, Construction, and Maintenance of Structures	Sep 1989
Instruction Report ITL-90-1	User's Guide: Computer Program for Design and Analysis of Sheet Pile Walls by Classical Methods (CWALSHT)	Feb 1990
Technical Report ITL-90-3	Investigation and Design of U-Frame Structures Using Program CUFRBC Volume A: Program Criteria and Documentation Volume B: User's Guide for Basins Volume C: User's Guide for Channels	May 1990
Instruction Report ITL-90-6	User's Guide: Computer Program for Two-Dimensional Analysis of U-Frame or W-Frame Structures (CWFRAM)	Sep 1990
Instruction Report ITL-90-2	User's Guide: Pile Group–Concrete Pile Analysis Program (CPGC) Preprocessor to CPGA Program	Jun 1990
Technical Report ITL-91-3	Application of Finite Element, Grid Generation, and Scientific Visualization Techniques to 2-D and 3-D Seepage and Groundwater Modeling	Sep 1990
Instruction Report ITL-91-1	User's Guide: Computer Program for Design and Analysis of Sheet-Pile Walls by Classical Methods (CWALSHT) Including Rowe's Moment Reduction	Oct 1991
Instruction Report ITL-87-2 (Revised)	User's Guide for Concrete Strength Investigation and Design (CASTR) in Accordance with ACI 318-89	Mar 1992
Technical Report ITL-92-2	Fiinite Element Modeling of Welded Thick Plates for Bonneville Navigation Lock	May 1992
Technical Report ITL-92-4	Introduction to the Computation of Response Spectrum for Earthquake Loading	June 1992